The Effect of Temperature on Bubble Size in a Lab-scale Flotation cell

Mandy Lokko

Department of Mining and Materials Engineering

McGill University

Montreal, Canada

February 2023

A thesis submitted to McGill University in partial fulfillment of the requirements of the degree of Master of Engineering

ABSTRACT

Flotation is a widely utilized mineral separation technique that is used to process large tonnages of low-grade and complex ores, which would otherwise be deemed uneconomical to exploit. This process exploits the differences in the hydrophobicity and bubble-particle interaction of the surfaces of the ore to achieve the separation of valuable minerals. This mainly surface-area-driven mechanism plays an essential role in flotation kinetics, as it drives the recovery function of the entire flotation process. The inclusion of bubble size measurements is important in modelling flotation cells as bubbles and bubble size are collectively an integral part of the flotation process. Due to seasonal temperature variations, temperature changes have been shown to affect overall flotation performance in many flotation plants located in temperate regions.

This work involved finding a suitable methodology to determine the effect on the Sauter mean bubble diameter or bubble size distribution in a Denver mechanical cell by varying the temperature of the pulp at different setpoints between a range of 5 °C and 40 °C. The methodology involved two processes whereby the bubble sizes were varied by altering temperature in a Denver mechanical flotation cell. The bubble sizes were captured and analyzed using the McGill Bubble viewer and an inbuilt McGill Bubble size Analyzer software respectively, to determine the bubbles' Sauter mean diameter (D_{32}). For the constituent of the pulp, two different frothers (MIBC and PPG 425) were selected to investigate their individual effects on the bubble size distribution under these temperature variations. The ranges specified for all the parameters were representative of industrial practice. The pulp primarily consisted of a frother solution (liquid-air phase system).

The results showed that the CCC_{95} values for both frothers were within the range of 10-15 ppm and 5-9 ppm for MIBC and PPG 425 respectively. The CCC_{95} was found to decrease after 1cm/s for both frothers. Furthermore, it was observed that the CCC_{95} changes with temperature. Temperature was shown to affect the bubble sizes. Specifically, above 10 °C, the differences in bubble sizes of both frothers were marginal due to the frother reaching its saturation at CCC_{95}.

Further tests at a lower CCC_X of 50% showed a marked difference in bubble sizes for both frothers. Overall, bubble size increased in the lower and higher temperature range of 20-40 °C. However, PPG 425 proved to be different as the D_{32} increased substantially at lower temperatures, specifically below 10 °C, which is indicative of the process water temperature within a typical Canadian plant where summer-winter fluctuation could typically show a 15 °C change in temperature.

RÉSUMÉ

La flottation est une technique de séparation des minéraux largement utilisée qui est utilisée pour traiter de gros tonnages de minerais à faible teneur et complexes, qui seraient autrement considérés comme non rentables à exploiter. Ce processus exploite les différences d'hydrophobicité et d'interaction bulle-particule des surfaces du minerai pour réaliser la séparation des minéraux précieux. Ce mécanisme principalement lié à la surface joue un rôle essentiel dans la cinétique de flottation, car il pilote la fonction de récupération de l'ensemble du processus de flottation. L'inclusion de mesures de la taille des bulles est importante dans la modélisation des cellules de flottation, car les bulles et la taille des bulles font collectivement partie intégrante du processus de flottation. En raison des variations de température saisonnières, il a été démontré que les changements de température affectent les performances globales de flottation dans de nombreuses usines de flottation situées dans les régions tempérées.

Ce travail consistait à trouver une méthodologie appropriée pour déterminer l'effet sur le diamètre moyen des bulles de Sauter ou la distribution de la taille des bulles dans une cellule mécanique de Denver en faisant varier la température de la pâte à différents points de consigne entre 5 °C et 40 °C. La méthodologie impliquait deux processus dans lesquels les tailles de bulles étaient modifiées en modifiant la température dans une cellule de flottation mécanique de Denver. Les tailles de bulles ont été capturées et analysées à l'aide de la visionneuse de bulles de McGill et d'un logiciel intégré McGill Bubble Size Analyzer, respectivement, pour déterminer le diamètre moyen de Sauter des bulles (D_{32}). Pour le constituant de la pâte, deux moussants différents (MIBC et PPG 425) ont été sélectionnés pour étudier leurs effets individuels sur la distribution de la taille des bulles sous ces variations de température. Les plages spécifiées pour tous les paramètres étaient représentatives de la pratique industrielle. La pâte consistait principalement en une solution moussante (système en phase liquide-air).

ACKNOWLEDGEMENTS

I would like to express my profound gratitude to Prof. Kristian Edmund Waters for giving me the rare opportunity to work on this project and for the successful completion of this thesis.

Within my research group of prolific resource persons, I was fortunate to have been guided by Mark Lepage, especially in giving me the overview or scope of this project, notwithstanding his continued support throughout the project. I would also like to acknowledge Mr. Chukwuma Obiajulu Collins for his strong technical and moral support for me throughout this project; his input was instrumental in the excellent delivery of all my results. I am thankful to Ronghao Li, who was my lab support and buddy especially throughout the pandemic; his encouragement and assistance in the lab was very needed throughout this difficult time. I gratefully acknowledge Dr. Ozan Kokkilic, Dr. Yue Tan, Dr. Luis Vinnett and Dzmitry Pashkevich and for their technical input.

The entire experimental setup and running of this project would not have been piloted without the extensive assistance of Mr. Raymond Langlois. I am sincerely grateful to him for being patient and putting in so much effort into making this project a reality as this project was a first of its kind. His technical experience is imprinted throughout the experimental process of this project.

I would also like to give a huge thanks to Aleksandra Djuric, who assisted me greatly, by giving me upmost priority, in the provision of the huge volumes of reverse osmosis water needed throughout this project, especially with all the complications throughout the COVID-19 pandemic. I would also like to give my sincere thanks to Barbara Hanley who was my strong support and guide: academic, family and friend; throughout my graduate studies. I would also like to acknowledge The National Sciences and Engineering Research Council of Canada (NSERC) for introducing and funding this novel collaborative project, of which I was given the opportunity to be a part of.

Finally, I would like to thank my mother, Angela Poku for supporting me throughout my studies despite her ill health, as her encouragement was very needed to inspire me to be persistent. Also, the memory of my late father Captain Christian Carl Lokko, continually inspired me to never give up, of which I am eternally grateful. I am also grateful to the rest of my family and friends for their genuine support throughout this study.

CONTRIBUTION OF AUTHORS

This research work primarily investigated the effect of temperature on bubble size during flotation in a lab-scale setting. The work presented was conducted in two parts to encapsulate: the development of a detailed experimental setup to measure the temperature effect on bubble size and to ascertain the effect of temperature on bubble size using the two main frother types. In addition, the impact of temperature on bubble size was correlated with bubble surface area flux to predict its consequential effects on flotation recovery. The contributions to this extensive work would be summarized in these actions: the conception or design of work, data collection, data analysis and interpretation, drafting of the thesis, critical revision of the thesis, and final approval of the version to be published.

The thesis, finally dubbed "The effect of temperature on bubble size in a lab-scale," was conceived and supervised by Prof. K. E. Waters and presented to Mandy Lokko to perform the investigation. The background was to answer a research question and observation in various mines in response to seeming different plant recoveries recorded due to the seasonal variations. Amongst the parameters contributing to flotation, this research only delved into the temperature effect on bubble size, while other parameters were designated to other persons.

The design of the work was a collaborative effort between Mr. Raymond Langlois and Mandy Lokko. First, Mr. Raymond Langlois provided his vast technical input into the design and construction of the heat exchange system (the use of the Isotemp bath circulator to vary the temperature with the Denver cell to impact bubble size). Subsequently, Mandy Lokko, the primary author, did all the experimentation, data collection, storage, and analysis.

The model employed for the data analysis to determine the Sauter mean bubble diameter (D_{32}) and the Critical Coalescence concentrations (CCC_{95} and CCC_{50}) is the Jan E. Nesset Model. Mr. Mark Lepage developed the MATLAB program embedded in the McGill Bubble size Analyzer used in performing image analysis on the captured bubbles. The statistical method employed to ascertain the effect of temperature setpoints on D_{32} was primarily the ANOVA method.

The thesis was drafted mainly by Mandy Lokko, the candidate. The drafted article was improved with the help of Mr. Chukwuma Obiajulu Collins, and Prof. K. E. Waters did a final critical revision. Prof. K. E. Waters gave the final approval for submission.

TABLE OF CONTENTS

LIST OF FIGURES

LIST OF TABLES

NOMENCLATURE

Symbol	**Description**	**Units**
d_b	Nominal Sauter mean bubble diameter	mm
D_{10}	Sauter mean bubble diameter	mm
D_{32}	Sauter mean bubble diameter	mm
D_l	Limiting bubble size	mm
BSD	Bubble size distribution	
E_A	Attachment efficiency	%
E_c	Collision efficiency	%
E_k	Collection efficiency	%
Es	Stability efficiency	%
J_g	Superficial gas velocity	cm s^{-1}
k	Flotation rate constant	s^{-1}
R	Recovery	%
R_c	Collection zone recovery	%
R_f	Froth zone recovery	%
S_b	Bubble surface area flux	s^{-1}
$S_{i,j}$	Relative floatability	Dimensionless
Efroth	A froth recovery efficiency factor	%
Ecol	Collection efficiency	%
CMC	*Critical Micelle concentration*	ppm
CCC	*Critical Coalescence Concentration*	ppm
ε_g	Gas holdup	%
ε_l	Water content	%
τ	Residence time	s
P	Mineral particles	

CHAPTER ONE: INTRODUCTION

1.1 Introduction

The ever-increasing complex mineralogy and occurrence of many low-grade ore reserves have economically brought about the evolution of technology in the treatment of these minerals (Kyzas *et al.*, 2019). Flotation is the most versatile separation technique employed in mineral processing for the selective recovery of valuable minerals. This separation process was discovered and commercially patronized at the onset of the 20th century (Ata, 2012). Flotation has been beneficial in mining and processing low-grade and complex ores that would have been considered uneconomical to exploit (Franzidis and Harris, 2010). Without flotation, many known metals and inorganic raw materials would be very scarce and costly because the processes used in extracting high-grade ores, which were considered simple, were used up (Kyzas *et al.*, 2019). Froth flotation was initially developed to treat sulfide minerals of lead, zinc, and copper and has expanded to treat nickel, platinum, and gold-hosting sulfides as well as non-sulfides such as oxides and some non-metallic minerals (Rao and Leja, 2004).

In flotation, the ore is mined, crushed dry, and milled wet, followed by reagent addition to create a slurry added to a flotation cell or unit. Air is purged through the slurry, and the mineral of interest is separated from the gangue and collected by floating to the top in an ideal situation (Franzidis and Harris, 2010). Froth flotation uses the differences in physicochemical surface properties of various minerals to achieve specific separation (Zhang, 2013). During the separation mechanism, bubble-particle interaction and bubble size are vital because they are surface area-driven processes. The surface area plays an essential role in flotation kinetics as it drives the recovery function of the entire process (Sovechles and Waters, 2015). Hence, the separation process's overall efficiency relies on the bubbles' size.

Consequently, bubble size measurements and modelling in flotation cells and controlling the generation of optimum bubble size ranges are required (Zhang, 2014). Some work has been conducted on bubble measurement and modelling in flotation. Still, none of these works have adequately accounted for principal variables, such as temperature, which affects the flotation process (Kracht and Finch, 2009).

Froth flotation facilitates the separation of valuable minerals from low-grade ore bodies through differences in hydrophobicity and bubble-particle interactions. Three main mechanisms are involved in recovering a valuable mineral from a pulp: the selective attachment to air, entrainment in the water which passes through the froth, and the physical entrapment between particles in the attached froth to air bubbles. Bubble size, which is controlled by a combination of bubble coalescence and break-up phenomena, plays an essential role in flotation kinetics as it is a surface area-driven process (Sovechles *et al.*, 2015). The generation of bubbles and stability of the froth is achieved using frothers. The attachment of minerals of interest to air bubbles is crucial and represents the bulk of the particles recovered as the concentrate.

Temperature plays an important role in temperate regions, where seasonal fluctuations exist, as it alters other parameters, such as pulp viscosity and density. Plants also operate where pulp temperatures vary from nearly 0 °C to 70 °C. Particle size and solid content vary widely, impacting pulp viscosity (Zhang, 2013). The solid content and the particulate nature of the pulp, which are affected by density and viscosity variations, determine the extent of bubble-particle interactions; thus, determining the effect of temperature on bubble size is desirable (James *et al.*, 1984). Consequently, the resulting impact on bubble size is of interest as many plants experience seasonal changes in water temperature or particle size changes as ore hardness, mineralogy and throughput fluctuate. Previous studies by Zhang (2014) investigated the effect of viscosity changes on bubble size in a mechanical flotation cell. However, determining the impact of temperature changes on bubble size in flotation would emphasize the temperature factor on the efficiency of the separation process and how it affects the recovery of a plant.

1.2 Thesis Objectives

The aim of this research was to investigate the effect of temperature on bubble size in flotation on a lab scale. The main objectives of this research are to:

- develop a detailed experimental methodology to aid in measuring and determining the effect of temperature on bubble size.
- establish the Critical Coalescence Concentrations (CCCs) and superficial gas velocity for the different frother types.
- establish the effect of varying temperatures on bubble size (D_{32}).
- investigate the frothers' performance with varying temperature.

CHAPTER TWO: LITERATURE REVIEW

2.1 Froth Flotation

Flotation is a separation process that uses natural variations in the surface properties of minerals (Wills and Finch, 2016). The flotation process depends primarily on the control of the pulp chemistry (Deglon *et al.*, 2000). Froth flotation separates valuable minerals from low-grade ore bodies through differences in hydrophobicity and bubble-particle interactions. The separation process exploits the differences in the surface properties of the minerals; if the surface is readily wetted by water, it is termed hydrophilic, but if it repels water, it is termed hydrophobic. The recovery of a valuable mineral from a pulp involves three principal mechanisms: the selective attachment to air, entrainment in the water which passes through the froth, and the physical entrapment between particles in the froth attached to air bubbles (Wills and Finch, 2016). The flotation process comprises three steps (i) the collision of air bubbles and mineral particles, (ii) mineral particles' adhesion or attachment to the air bubbles, and (iii) the subsequent transport of the stable particle-bubble aggregate to the froth phase.

The valuable mineral of interest is typically transferred to the froth during flotation, leaving the gangue in the tailings. This process is known as direct flotation, and the opposite is termed reverse flotation, where the gangue is floated instead (Wills and Finch, 2016). Several reagents are used in the flotation process, which has been categorized into frothers, modifiers, and collectors (Chander and Nagaraj, 2007). Not all valuable particles that report into the froth phase are recovered; some particles are detached from the bubbles because of coalescence. Indeed, 85-90% of the particles that reach the froth-pulp phase return to the collection zone as the thin liquid films between bubbles rupture during coalescence (Chipfunhu *et al.*, 2019). Therefore, froth recovery and froth stability influence the recovery of the flotation process entirely. An overview of the flotation process is shown in Figure 2.1.

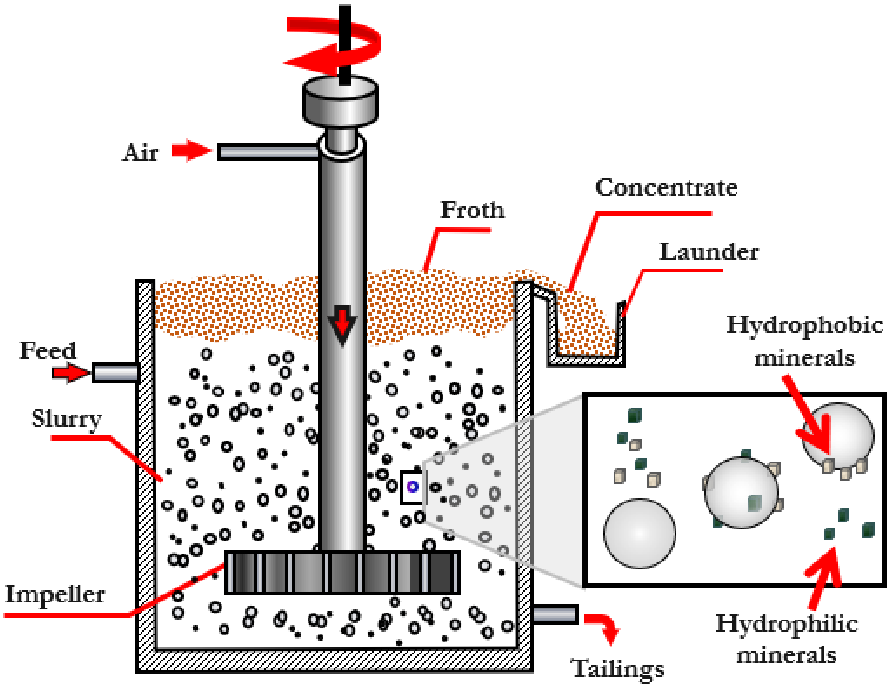

Figure 2.1: A general overview of flotation in a mechanical cell. Modified from Wills and Finch (2016).

Here, the feed is introduced into the flotation cell. The impeller provides turbulence for contact or collision between the bubbles and the particles. The mineralized bubbles (hydrophobic minerals) rise and are collected as a concentrate, while the non-valuable minerals constitute the tailings stream. There are three phases in flotation: solids, water (liquid), and air. These phases interact with the system's physical and chemical variables. The three sub-processes involved in the flotation process are termed collection, and the collection efficiency (E_{col}) is given in Equation 2.1 (Derjaguin and Dukhin, 1993; Chipfunu *et al.*, 2019).

$$E_{col} = E_c E_a E_s \tag{2.1}$$

where E_c, E_a and E_s represent the collision efficiency, the adhesion or attachment efficiency, and the stability efficiency respectively. In addition to the above equation, a froth recovery efficiency factor, E_{froth} may also be applied to accommodate the froth effect on the flotation recovery (R), Equation 2.2:

$$R = f E_{col} E_{froth} \tag{2.2}$$

The collision efficiency is not only influenced by long-range hydrodynamic forces, but it is also a function of the physicochemical properties of the mineral particles and the hydrodynamics (e.g., bubble rise velocity, impeller speed, bubble size, and others.). As bubbles and particles approach each other closely, short-range interfacial forces become predominant. These forces aid in the rupture of the thin liquid film between the particle and the bubble, thereby promoting the formation of the three-phase line of contact for successful particle-bubble attachment. The attachment efficiency (E_a) is controlled surface forces which are primarily a function of particle hydrophobicity. The particle-bubble aggregate upon attaching must be stable, and the attachment forces must be greater than the disruptive detachment forces, which constitutes stability efficiency, E_s .

The stability of particle-bubble aggregate, a function of surface forces and hydrodynamics, is greatly influenced by the contact angle, particle size (Inertial forces), and pulp viscosity. In conclusion, the three flotation sub-processes are conditions necessary for flotation to happen effectively; and they are influenced by flotation reagents added to enhance the selectivity. Additionally, the correct selection of reagents would impact the grade, recovery, economics, and selectivity of the flotation process (Chipfunhu *et al.*, 2019).

2.2 Flotation Reagent

Flotation reagents belong to three significant groupings: frothers, collectors, and modifiers (Chander and Nagaraj, 2007). Their development over the past centenary was done in line with flotation over that same period. In the 1920s, up to 10 kg/ton of different insoluble oils were used. In addition, other types of reagents such as soaps, oleic acid, copper sulfate, lime, soda ash, cresylic acids, sulfur dioxide, aldehydes, esters, aliphatic alcohols, pine oil, and esters were introduced to achieve better recoveries (Chander and Nagaraj, 2007). There was a significant development from 1921-1950 in the rubber and agriculture flotation industry, where smaller amounts of reagents (less than 0.5 kg/ton of ore) were used. Xanthates, sodium cyanide, dithiophosphate, and petroleum sulphate were among the collectors utilized during this period. Hence, from 1951 until the present, the development of flotation reagents targets a specific design approach. Some examples of such reagents include alkoxycarboyl thiourea, dialkyl thionocarbamates, hydroxamates, alkoxycarbonyl, amongst others. As mentioned previously, flotation reagents are categorized into three groups based on the functionality or purpose of chemical reactions. They make up the flotation triangle, as shown in Figure 2.2 (Chander and Nagaraj, 2007).

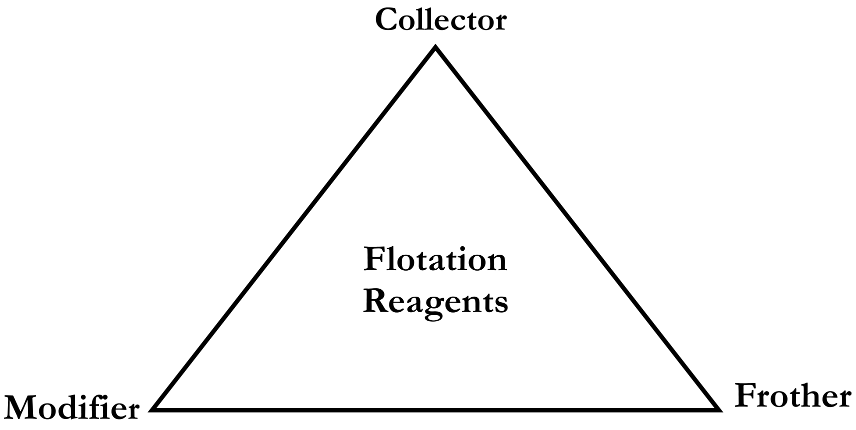

Figure 2.2: Flotation reagent triangle adapted from (Chander and Nagaraj, 2007).

Flotation can occur without any reagent in naturally hydrophobic minerals with a water contact angle greater than zero. However, some hydrophobic and partially hydrophobic minerals like molybdenite, and carbonaceous materials, which include certain metals and carbon-bearing shales, do not float in pure water. With the addition of frothers in the form of inorganic electrolytes or organic compounds, these types of minerals can be floated (Drzymala and Kowalczuk, 2018). The addition of chemical reagents such as collectors and frothers quintessentially controls flotation performance (Zhou *et al.*, 2016). Adding reagents such as frother, depressant, and collectors in particular quantities aids in improving the process. When these reagents are added, the physical and chemical properties of the flotation process will be altered (Chander and Nagaraj, 2007). For instance, by increasing the frother quantity within the pulp, bubble size decreases, which increases the separation efficiency of the valuable minerals (Hayono *et al.*, 2016). Frothers are neutral molecules that are grouped into soluble and partially soluble surfactants. Frothers function by aiding in the generation and preservation of fine bubbles and generating a stable froth zone at the top of the pulp within the cell (Chander and Nagaraj, 2007).

Collectors are often classified into ionic (anionic or cationic) and non-ionic surfactants, and additionally sulfydryl, thio, thiol, nonthio, nonthiol, soluble, insoluble, oily hydrolyzable, ionizable, amongst others (Chander and Nagaraj, 2007). Collectors are organic compounds that make mineral surfaces water-repellent when they adsorb to specific minerals (See Figure 2.3), thereby decreasing the stability of the hydrated layer and separating the mineral from the air bubble to allow the particle to attach to the bubble generated within the pulp. To render a mineral hydrophobic, time is allowed for adsorption during agitation when the collectors are added in the conditioning period, thereby reducing induction time (Wills and Finch, 2016). The primary role of a collector is to render mineral surfaces sufficiently hydrophobic to encourage the probability of mineral-bubble attachment. However, if a mineral is naturally hydrophobic, it can be floated without adding a collector (Chander and Nagaraj, 2007).

Several hundred collectors have evolved over the years in flotation. They may be non-ionizing compounds that are highly hydrophobic and insoluble, often used with naturally hydrophobic minerals like molybdenite and coals to increase floatability, known as assisted flotation. They may also be ionizing and soluble; hence, they are classified by the type of ion, cationic or anionic major application, sulfide, or non-sulfide mineral (Wills and Finch, 2016). Collector adsorption happens through various reactions involving the collector and the mineral. The driving force for adsorption relies on the solubility product of the mineral-reagent complex and the reactivity of the collector. The formation of salt between the cation in the mineral and the collector, X^-, is shown in Equation 2.3 and expressed as a solubility product in Equation 2.4 (Chander and Nagaraj, 2007).

$$M^{Z+} + zX^{-} = MX_{z} \tag{2.3}$$

The solubility product now is

$$K_{sp} = [M^{z+}][X^{-}][X^{-}]^{z} \tag{2.4}$$

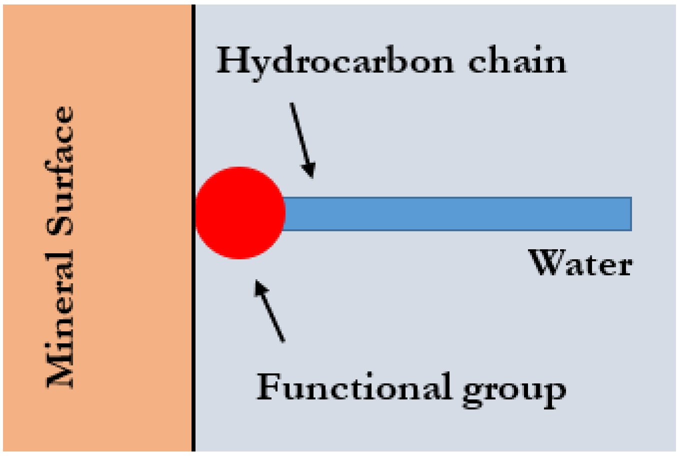

Figure 2.3: An image depicting the adsorption of a collector on a mineral surface. Modified from Wills and Finch (2016).

Modifiers are often described as pH modifiers (or regulators), depressants, dispersants, activators, deactivators, promoters, froth modifiers, viscosity modifiers, gangue-control reagents, and slime-binding reagents according to said functionality. Modifiers are not discussed much in flotation literature, and there is no specific classification for them. It would be complicated to classify modifiers because, within a flotation system, an individual collector can have multiple functionalities. This functionality, however, varies from system to system. A single modifier can have a wide range of applications; hence, the broad term modifier is preferred as the third apex of the flotation reagent triangle. Modifiers aid in selective flotation based on the complexity of mineralogy, and they have wide usage in flotation. The industry's most common, economic, and easily accessible inorganic compounds and natural modifiers are highly patronized (Chander and Nagaraj, 2007).

2.2.1 Frothers

The importance of frother usage in flotation has been identified and established over a long period. Its addition is nearly universal in mineral flotation plants and generally aids in producing smaller bubbles and improving the overall flotation kinetics (Cho and Laskowski, 2002). Flotation kinetics entails several mass transfer processes. Some occur in the pulp phase, that is, particle-bubble interaction and attachment and transport of bubble-particle aggregate to the froth phase). Likewise, the mass transfer could also exist in the froth phase, that is, the recovery of the particle from the froth phase to concentrate launder (Cho and Laskowski, 2002). These processes depend highly on bubble size and froth stability (Cho and Laskowski, 2002). Therefore, a reduction in bubble size (fine bubbles) is essential in increasing flotation kinetics: the reduction increases the total number of bubbles, hence the overall surface area and increased collisions with particles within the pulp (Wills and Finch, 2016).

However, the mechanism by which frother controls bubble size is not widely known and not directly related to surface tension reduction. A common explanation is the prevention of bubble coalescence (Laskowski, 2003), but this mechanism of frother action relevant to bubble generation (as opposed to froth formation) remains obscure (Cho and Laskowski, 2002). According to Tan *et al.* (2018), frothers are a class of surface-active agents that are used in mineral flotation. They are basically non-ionic heteropolar surfactants that consist of hydrophilic or polar groups, commonly O and OH, and hydrophobic or non-polar groups, usually hydrocarbon chains. Water dipoles usually interact (H-bond) with the polar groups of the frother and not with the non-polar groups (Zhang, 2012).

Therefore, the heteropolar structure of the frother molecule effectuates the adsorption at the air-water interface (bubble surface), with the non-polar groups oriented towards the airside of the interface. The polar groups are oriented toward the water side in the pulp or collection zone, as shown in Figure 2.4a, which influences collision and attachment processes in flotation (Zhang, 2012; Chipfunu *et al.*, 2019). Frothers are used to enhance the production of fine bubbles and to stabilize froth (Cho and Laskowski, 2002).

Frother have two main functions, namely: dispersion of air into fine bubbles and its preservation to aid in the gathering of the mineral particle; and the stabilization of the froth phase to assist in the recovery of the accumulated mineral particles at the overflow (Wills and Finch, 2016; Chipfunhu *et al.,* 2019). These two main functions have been explicitly subdivided into three principal functions: (i) aid in the formation and preservation of small bubbles, (ii) reduce bubble rise velocity, and (iii) stabilization of froth (Tan *et al.*, 2018; Klimpel and Isherwood,1991; Wills and Finch, 2016). The agglomeration of these small fine bubbles at the top of the pulp forms a stable froth, enabling the separated particles to be collected as the float fraction in the overflow (Wills and Finch, 2016). In industry, frothers are usually determined and selected based on their chemistry, either alcohols or polyglycols (Chander and Nagaraj, 2007).

Two commercially used frother types are alcohols and polyglycols (Gupta and Yan, 2016). Alcohol frothers generally contain a single hydroxyl (OH) group comprising 5-7 carbons, either straight or branch chained. MIBC (Methyl Isobutyl Carbinol) is one of the most common in this group. Polyglycol frothers have a large class with varying molecular weight and structure. Flottec 150 (F150) and Dowfroth 250 (DF250) are some notable examples of this group (Klimpel and Isherwood, 1991; Laskowski, 1998; Zhang, 2012; Zhang *et al.*, 2013). In their application, alcohol frothers are specialized in selective fine particle recovery, whereas polyglycols focus on selective coarse particle recovery (Klimpel and Isherwood, 1991; Zhang *et al.*, 2013).

2.2.2 Frother Types

As stated previously, frothers are a group of surface-active agents extensively utilized in flotation of minerals. Their main functions are to form and maintain small bubbles, decrease bubble rise velocity, and sustain froth (Tan *et al.*, 2018). Currently, alcohols and polyglycols are the two main frother types used on a commercial scale. A third type includes alkoxy substituted paraffins. Previously, some natural oils like pine oils were utilized as frothers for flotation, but they also had collecting abilities that inhibited process selectivity, as both collecting and frothing characteristics in a single reagent can render selective flotation challenging (Wills and Finch, 2016). Pugh (2007) established that frother performance relies on its chemical structure. Increased branching decreases maximum floatable particle size, whereas increased branching increases selectivity (Klimpel and Hansen, 1988; Klimpel and Isherwood, 1991). The general chemical formula for both frother types is indicated as $C_nH2_{n+1}OH$ for alcohols; and $R(X)_yOH$ for polyglycols, where

R=H, or $C_nH_{2n}+1$ and X commonly represents propylene oxide, PO (-C_3H_6O-) or ethylene oxide, EO (-C_2H_4O-) which are polypropylene glycols and polyethylene glycols, respectively (Tan *et al.*, 2018). Alcohol frothers have a chain length of 5-8, and the molecular weight (MW) of a polyglycol and their ethers is between the 200-425 range (Chander and Nagaraj, 2007).

The frothers' structure can be found in either a branched, aromatic, cyclical, or liner form. This alcohol frother type also exhibits sensitivity to pH changes, has relatively low water solubility, and a kinetic rate with a corresponding change in frother dosage (Klimpel and Isherwood, 1991). Aliphatic alcohols such as methyl Isobutyl Carbinol (MIBC), 2-ethyl hexanol, and hexanol have been in existence industrially for decades. Aliphatic alcohols are characterized by less tenacity, more brittle froths, and low water retention than other frother groups (Klimpel and Isherwood, 1991). It has been observed that aliphatic alcohols seemingly show extremely high rates of flotation at lower dosages in plant frother quantification experiments. However, when the dosage is increased further, they exhibit an extremely high or pass the maximum flotation rate, then fall rapidly afterward (Klimpel and Isherwood, 1991). This behaviour indicates that an increase in frother dosage which seemingly corresponds to an increase in recovery in a flotation cell of fixed volume, may not always be the case.

Alcohol frothers are more effective at assisting selective fine particle recovery than polyglycol frothers due to their differences in solubilities, surface activity, and diffusion rates (Zhang *et al.*, 2013). Although alcohol frothers are considered to have very low solubility contrary to glycols that are completely miscible with water, at the low concentrations used in flotation solubility is not a limiting factor in selecting a frother selection for specific use (Chander and Nagaraj, 2007). The two most commonly patronized families of this frother type are polypropylene glycol methyl ethers and polypropylene glycols (Klimpel and Isherwood, 1991). Both polypropylene glycols and polypropylene glycol methyl ether frothers exhibit much-reduced sensitivity to pH variations (Chander and Nagaraj, 2007). Polyethylene glycols (also known as polyethylene glycol alkyl ethers, polyoxyethylene alkyl ethers, alcohol ethoxylates, and alkyl mono ethers of polyoxyethylene glycols) comprise two parts, the ethylene oxide (ethoxy, EO) group ($-C_2H_4O^-$) which makes the compound hydrophilic by the -O- linkage and the alkyl chain ($-C_nH_{2n+1}$), which is hydrophobic (Tan *et al.*, 2018). For small values of n (n = 1,2), and (n = 3, 4 .... 8). polypropylene glycol methyl ethers range from highly miscible in water to partially soluble as n increases, respectively (Klimpel and Isherwood, 1991).

The structure of both the EO and alkyl chains controls the surfactant properties. With the simplified formula as $Cn(EO)_l$, by varying n and l, that is, the ratio of hydrophobic to hydrophilic groups, PEGs can range from completely miscibility with water to partially soluble (Laskowski, 2001; Tan *et al.*, 2018). The ability and ease to vary solubility and molecular weight within the same chemical analog of these frother types offer maximum flexibility in reference to improved water retention, bubble size and preservation, and deeper froth depth character (Klimpel and Isherwood, 1991). The froths from these frothers are tightly knit bubbles that are more persistent than those of alcohol. With the same dosage of frother, the recovery capability for polyglycol frothers is usually higher than aliphatic alcohol frothers on the contrary. However, with a further increase in dosage, the glycols do not show nearly as strong a rate as the aliphatic alcohols (Chander and Nagaraj, 2007).

2.3 Frother chemistry and structure

As stated earlier, the principal functions of frother give a reflection of their molecular structure, which impacts flotation. For instance, different chemistries can result in different flotation recovery depending on particle size (Klimpel and Isherwood, 1991; Wills and Finch, 2016; Tan *et al.*, 2018). These functions reflect their molecular structure, which impacts flotation; for example, different chemistries give different flotation recovery depending on particle size (Klimpel and Isherwood, 1991). The choice of frother for a given duty remains empirical, but progress is being made in developing tests to characterize frothers to aid selection (Laskowski, 2003; Cappuccitti and Finch, 2008). Several studies linking frother functions to frother structure have been well documented (Zhang *et al.*, 2012; Kowalczuk, 2013; Finch and Zhang, 2014; Corin and O'Connor, 2014; Tan and Finch, 2016). The development of new frother chemistries attuned to frother performance- for example, improved fine or coarse particle recovery- has been conducted in addition to the design of frother blends (Zhang, 2012).

Frother properties rely on several factors, such as concentration and ability to interact with water, solids, modifiers, collectors, and structure. Due to these factors, frothers can be classified (Drzymala and Kowalczuk, 2018). These classifications include pH sensitivity, (ii) solubility, (iii) frothing/collecting properties, and (iv) selectivity/frothing power (Drzymala and Kowalczuk, 2018; Khoshdat and Sam, 2011). Other categories look at how the frother acts as a collector and the ability of frothers to float particles according to their size (Drzymala and Kowalczuk, 2018; Laskowski, 2004).

Another classification considers the chemical structure and divides frothers into alcohols and non-alcohols, as shown in Table 2.1. The alcohol frothers can be further divided into classes depending on the alcohol structure. The non-alcohol frothers can also be divided into organic and inorganic. The non-alcohol organic frothers, instead of –OH, contain bonded oxygen in their structure. In their native state, frothers can be solid, such as terpineol with a melting point of 40 °C, inorganic salts, liquid (most organic frothers including polyglycol ethers), and gas (ammonia). Hence, Pugh (2007) indicated that the performance of a frother is typically reliant on its chemical structure. An example of two commonly used polyglycol and alcohol frothers can be seen in Figure 2.4b.

Frothing characteristics rely on the frother structure, for example, the relative strength of the hydrophobic or non-polar groups to the hydrophilic or polar groups. With any individual frother family, the length of the hydrophobic to the hydrophilic groups can be adjusted by varying the number of Propylene Oxide (PO) or Ethylene Oxide (EO) groups in the case of Polyglycols and or the number of -CH_2- groups in the alkyl chain for both Alcohols and Polyglycols. The change in the relative length of the hydrophobic to the hydrophilic group in the molecule is described as the hydrophile-lipophile balance, or HLB (Laskowski, 2003).

The measure of structure seeks to express the heteropolar nature of frothers. Hence, hydrophile-lipophile balance (HLB) was recommended and used as a means of measurement. The HLB number is a measure of the degree of hydrophobicity and hydrophilicity of a surfactant, and the HLB number is altered when the ratio of the hydrophobic groups to the hydrophilic groups is varied (Laskowski, 2003; Rao and Leja, 2004; Pugh, 2007; Zhang 2012). The structural properties of frothers, such as the length of the hydrocarbon/alkyl chain and the number of the PO groups in the HLB theory, correspond with flotation performance. As a result, the frother's functions may have a close correlation with the HLB number. Therefore, the measurement of the frother's functions is referred to as frother characterization (Zhang, 2012).

Table 2.1: Typical frothers used in the industry adapted from Chander and Nagaraj (2007)

Frother	Structure	Uses
Aliphatic alcohols	$R-OH$ 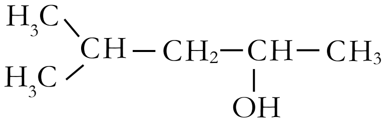 $(H_3C)_2CH-CH_2-\underset{\substack{\mid\\ OH}}{CH}-CH_3$ e.g MIBC $R-O-C_3H_6-OH$	Widely used
Poly (ethylene) or poly (propylene) glycols and their monoethers	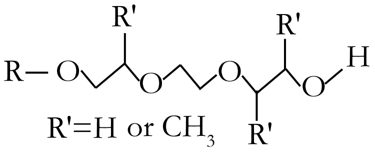 $R'=H$ or CH_3 $R=H$ or higher alkyls	Widely used
Alkoxy compounds	$(R-O)_x-R$ e.g Triethoybutane	Widely used
ketones	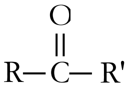 $R-\overset{\overset{O}{\parallel}}{C}-R'$	Minor amounts in aliphatic alcohol frothers
Aldehydes	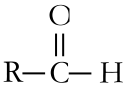 $R-\overset{\overset{O}{\parallel}}{C}-H$	Minor amounts in aliphatic alcohol frothers
Esters	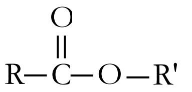 $R-\overset{\overset{O}{\parallel}}{C}-O-R'$	Minor amounts in aliphatic alcohol frothers
Pine oil	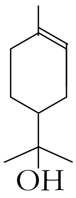	Limited use
Cresols (isomers)	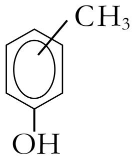	Limited use

As discussed in the above paragraphs, frothers are mostly heteropolar compounds that consist of a polar part (hydrophilic) and a non-polar part (hydrophobic). The hydrocarbon chain of the non-polar part is characterized by either a straight, cyclic, aromatic, or branched chain (Nassif, 2014; Laskowski, 2003). In the case of alcohols, the OH group represents the hydrophilic part; but could comprise alkoxy ($O–C_nH_{n+1}$) groups in the case of polyglycols. The different polarities give the frother molecule its property to adsorb at the air-water or bubble surface, with the hydrophobic group on the air side and the hydrophilic group on the water side as shown in Figure 2.4a (Finch *et al.,* 2008, Sweet *et al.*, 1997).

It has also been indicated that the maximum floatable particle size decreases by increasing branching, which reduces the maximum floatable particle size with increasing selectivity (Klimpel and Hansen, 1988; Klimpel and Isherwood, 1991). In the case of PEG groups, they are between partial solubility to complete miscibility with water. With the generic equation as $C_n(EO)_l$, the ratio of hydrophobic to hydrophilic groups shows the degree of solubility. Research has also shown that the structure of PEGs affects their properties. For instance, the critical micelle concentration (CMC) and surface tension decrease with increasing EO and alkyl chain length. Also, increasing alkyl chain length decreases surface tension (Tan *et al.*, 2018).

Szyszka (2018) suggested that there is an optimal molecular weight above which froth stability begins to decrease. At this supposed optimal weight, froth stability is also maximized; subsequently, increasing the molecular weight of Polypropylene Glycol (PPG) corresponds to an increase in froth volume produced (Zhang, 2012).

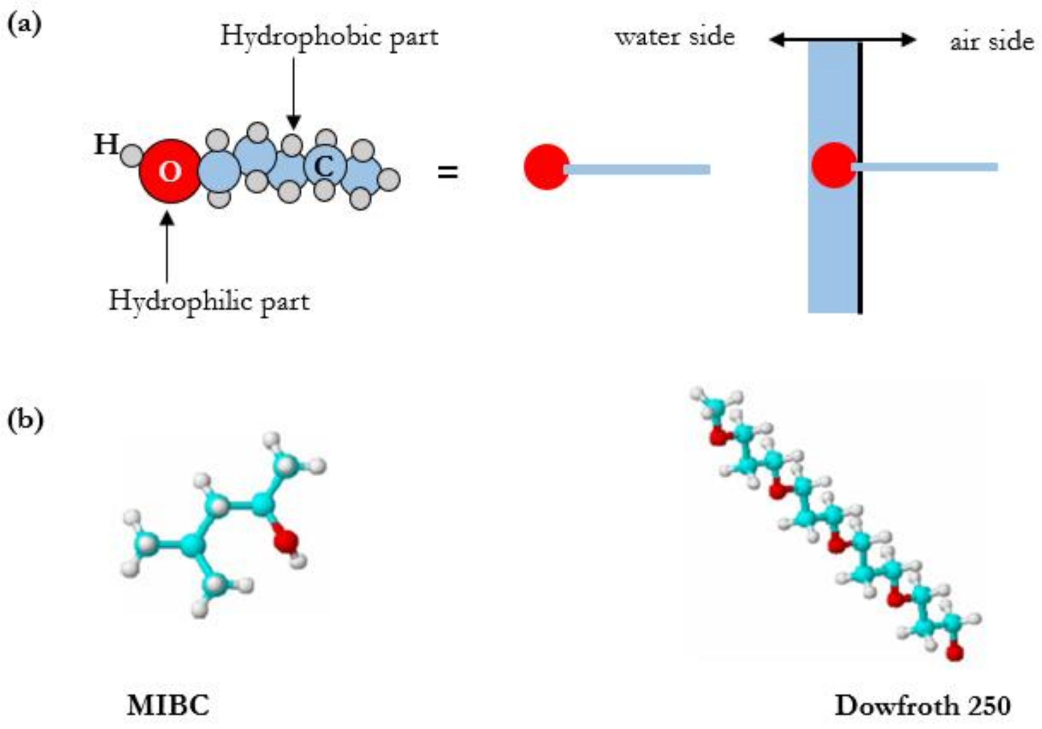

Figure 2.4: Diagram showing the general structure of frother (a) showing mixed polarity (left) and orientation at the air-water interface (right). (b) Examples of two common frothers (Left) alcohol and (right) polyglycol. Adapted from Finch *et al.* (2008).

2.3.1 Effect of frothers

Frothers are quintessentially added to aid in forming and conserving fine bubbles through coalescence inhibition and break-up phenomena (Sovechles *et al.*, 2016). That is to say; frothers are used to boost the formation of fine bubbles and stabilize froth (Laskowski, 2001). In addition to the previously mentioned functions of frother, frother has other roles, such as increasing gangue removal from the collected minerals by draining water from the inter-bubble spaces within the froth. The altering of surface-related properties of water, such as surface tension, viscosity, and coalescence, gives rise to the two main functions of frother in flotation: an increase in froth stability and bubble size reduction. These functions were asserted by Laskowski (2003), who was one of the main persons to make this discovery (Gélinas and Finch, 2007).

Frother usage is essential in flotation performance. It impacts the recovery and grade of mineral particles that report to the froth as the concentration for the mineral of interest (Comley *et al.*, 2002; Zhang, 2012). In the flotation industry, the blending of frothers is highly accepted and practiced (Zhang *et al.*, 2013). The purpose of combining two frothers is to improve control within the process (Gélinas and Finch, 2007). In current years, the combination of two frothers has become more noticeable in operations. With the knowledge that frother provides two main functions: reducing bubble size and stabilizing froth, independent control over both functions could be achieved with a dual frother system. Therefore, this independent control is challenging to attain with just one frother type since the functions of frother are concentration dependent. Zhang (2012) opined that blending two different frother classes would result in an optimum recovery coupled with good selectivity. In addition, blending frothers results in the attainment of air dispersion and froth stabilization. It has been identified that polyglycol frothers target selective coarse particle flotation, whereas alcohol frothers are more suited for selective fine particle recovery. However, combining the two classes of frothers is recommended as the optimum for high recovery with good selectivity (Zhang *et al.*, 2013).

2.4 The role of frother in bubble formation and bubble coalescence

Frothers have a paramount role in the flotation of mineral or solid particles as they enable the formation of froth or foam and further modify the structure of films between bubbles and solid particles and bubbles (Drzymala and Kowalczuk, 2018). Frothers act by reducing bubble size and increasing the number of bubbles in a solution or pulp and, consequently, the number and surface area of bubbles produced within the pulp (Nesset, 2011; Wills and Finch, 2016). Once adsorbed, the frothers tend to form a tight liquid film around the bubble, varying thickness depending on frother chemistry. The liquid film is attributed to hydrogen bonding between the hydrophilic group of the frothers and water molecules. Frothers are believed to act on bubbles by retarding and preventing coalescence, thereby preserving a bubble's size, which mainly occurs at creation sites (Harris, 1982; Hofmeier *et al.*, 1995, Comley *et al.*, 2002).

Bubble break-up and bubble coalescence are two mechanisms that exist within a pulp. In an instance where a single bubble in water is subjected to some level of turbulence, the presence of a frother will play a part in the bubble's ability to disintegrate into smaller bubbles. The breakup will also impact the ability of the resulting product bubbles to reunify into larger bubbles, thus coalescence. Frothers, will concentrate at the air-water interface and impact the near-interfacial and interfacial properties of the bubble. Frother molecules will attach to the air/ water interface with its hydrophilic end (OH or related group) on the water side and its non-polar or hydrophobic part on the air side, as it is a hetero-polar structure (Nesset, 2011). Coalescence inhibition by frothers is a coalition of stabilization of a water layer on the bubble surface and an increase in the firmness of bubbles (Nesset, 2011). The discussion of coalescence depends on what process is the focus. What prevents coalescence at bubble formation seems easier to explain by the 'water layer' idea, but coalescence prevention in the foam can be explained by the rigidity idea and the action of particles (Cappuccitti and Nesset, 2009).

The role of frothers in facilitating bubble break up is even less well understood. It has been proven that bubble size (the Sauter mean size, D_{32} or nominally D_b) in the pulp phase is directly proportional to the ppm concentration of frother in the aqueous phase of the pulp. The frother type and concentration, bubble generation system, air rate, and viscosity, amongst other factors, determine the population of bubbles in a cell or bubble size distribution (BSD). Increasing frother quantity decreases the bubble size parameter, D_{32}, and dramatically changes the shape of the bubble size distribution (BSD). The BSD is less bi-modal and narrower as the dosage is increased. Hence, the optimum relation between the BSD and the particle size distribution can be produced by tuning principal variables, as there is control of the BSD within a flotation cell. As a result, coarser particles will be efficiently captured by larger bubbles and smaller particles by smaller bubbles (Cappuccitti and Nesset, 2009).

Although frothers reduce bubble size, salts such as NaCl are also known to reduce bubble size as well, despite increasing surface tension as opposed to frother, which does the reverse (Quinn *et al.,* 2007; Bournival *et al.,* 2012; Sovechles *et al.,* 2016). This may be due to uneven concentration causing the dynamic nature of surface forces over the bubble surface at the point of injecting air into the solution in which frother is randomly distributed. In addition, an unequal concentration of surfactant on the surface of the bubble at the point of air injection in the frother solution that gives rise to a resultant force from surface tension gradients rather than an entire decrease in surface tension may be a plausible reason (Zhou *et al.*, 2016). Hence the instabilities caused on the surface of the bubble cause bubble break-up when there is enough mechanical energy impact into the setup. With the increase of frother dosage into a gas-liquid mixture, there is an observable decrease of the distinctive bubble size (D_{32} or D_{10}) to a limiting value. Also, there will be a change in the shape of the frequency distribution of the bubble size population. From zero frother to higher frother concentration, the BSD and average bubble size will be characterized by a bi-modal distribution and larger bubble size, which depreciates to a much narrow BSD and smaller bubble size, respectively, as shown below in Figure 2.5.

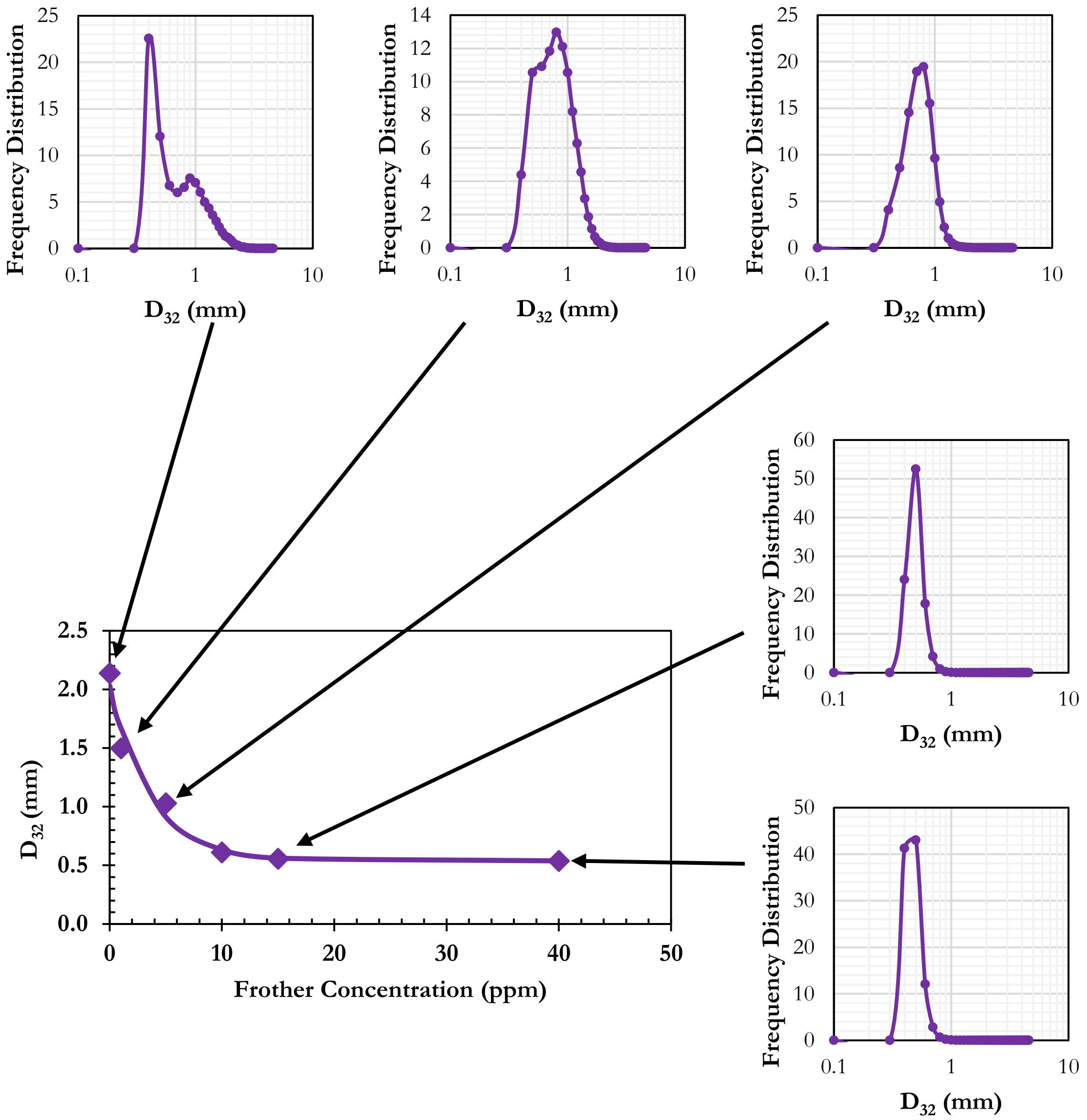

Figure 2.5: Diagram showing changes in bubble size distribution with increasing frother concentration[1].

2.5 Function of bubbles/ Role of bubbles in flotation

Froth flotation is a common separation process, yet essential in separating and recovering minerals of interest from an ore body. It utilizes air bubbles either in a mechanically agitated cell or a column. As bubbles are instrumental in the separation, factors such as bubble size generated and corresponding surface area contribute immensely to separation efficiency. Consequently, bubble

---

[1] This work
Frother: MIBC
Air rate: 1.5cm/s

size is a function of other factors such as frother type and concentration, air flow rate, gas density, impellor design and speed, pulp temperature, water quality, and type of chemicals within the pulp (Nesset *et al.,* 2007; Sovechles *et al.,* 2016). Therefore, bubble properties are affected by frother type and concentration (Nesset, 2011).

The rupture of thin liquid films separating two adjacent bubbles is one of the major reasons for two adjacent bubbles coalescing in the froth. Coalescence happens when the liquid content in the froth drops below a critical value. Particles and surfactants' presence seemingly tend to have a detrimental effect on the film rupture. It is assumed that once the thin film reaches its equilibrium thickness, the probability of the film failing is governed mainly by disturbances in the froth without the influence of particles attached to the film, though this has not been proven experimentally. Bubble coalescence was attributed to mechanical perturbations such as bubble oscillation and vibrations. Bubble coalescence will happen due to the presence of hydrophobic particles. As can be seen in Figure 2.6, when a spherical particle penetrates a foam film and conjoins the two interfaces, it will attempt to migrate toward a central position to meet the contact angle requirement. If the contact angle is less than a critical degree of wetting, a stable orientation will occur, and the film life will be prolonged. In addition, when the bridging particle has a contact angle more than the critical degree of wetting, the particle will readily wetted through both sides of the lamella, resulting in the film rupture. The critical degree of contact angle at which film failure occurs can be as low as 75° depending on particle size, the number of particles, shape, and the separation distance between the particles inside the film. To facilitate particles' attachment to bubbles and pass successfully to the concentrate, a contact angle of 30-50° is mostly adequate. It is uncommon to have a froth that has particles with high hydrophobicity, except for inherently hydrophobic minerals (Ata, 2012).

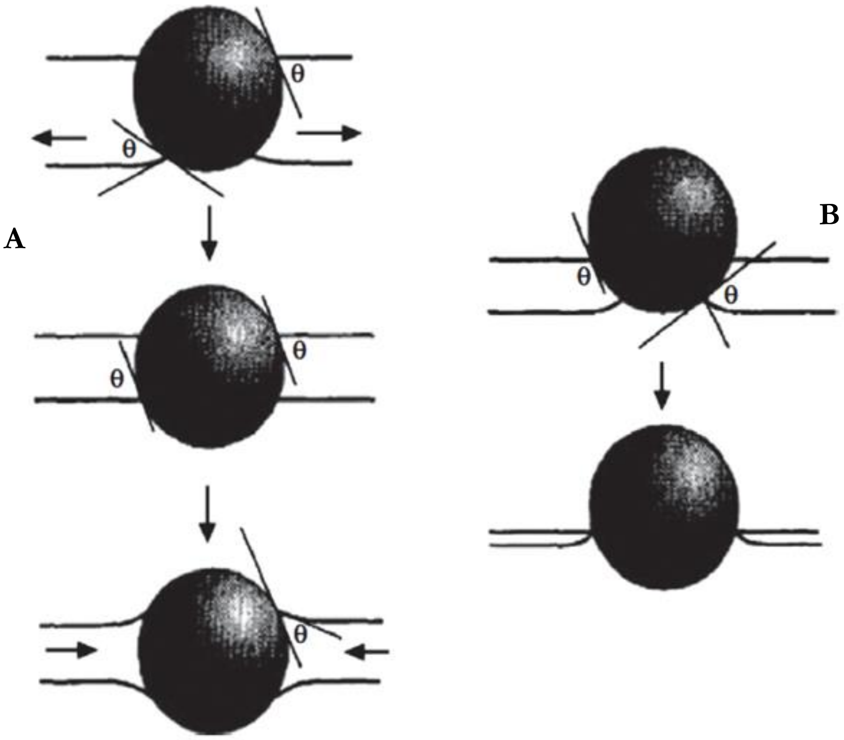

Figure 2.6: Bridging particle behaviour in a foam depicting contact angles (a) Moderately hydrophobic, (b) highly hydrophobic particle (Ata, 2012).

2.5.1 Bubble Surface Area Flux

It has been determined that bubble surface area flux, S_b, is the variable that gives a more general description of the aeration condition in flotation cells, both column and mechanical. S_b is defined as the bubble surface that flows across the cross-sectional area of the cell per unit time, is expressed in terms of d_b and J_g in Equation 2.5

$$S_b = \frac{6J_g}{d_b} \tag{2.5}$$

Various research has been conducted to evidence the relationship between S_b and the metallurgical variables, recovery, and grade. Models have been formulated to show that recovery R increases as the flotation rate constant, k, and residence time, τ, of the mineral particles increase and as cell mixing decreases (López-Saucedo *et al.*, 2012), as shown in Equation 2.6.

$$R = f(k, \tau, \text{mixing}) \tag{2.6}$$

The rate constant k is also dependent on the floatability of the mineral particles P, the aeration and hydrodynamics conditions existing within the cell S_b, and the characteristics of the froth zone R_f, as indicated in Equation 2.7:

$$k = PS_bR_f \tag{2.7}$$

Equations 2.5-2.7 clearly show that small bubbles enhance recovery if they are not smaller than approximately 0.2–0.4 mm. Research has strongly indicated that S_b is an essential parameter of the three-phase dispersion (López-Saucedo *et al.*, 2012). Sauter mean bubble diameter (D_{32}) and bubble surface area flux (S_b) are correlated to the metallurgical performance in terms of concentrate grade and recovery. Bubbles collected are currently measured with the McGill bubble viewer, and bubble size (D_b) characterizes the entire size distribution from the captured images (Gomez and Finch, 2007).

2.5.2 Bubble size measurement

The measurement of bubble size is deemed an inexact science. However, the change in frother concentration can be presently represented with a distribution of sizes and shapes, where the distribution could be normal, log-normal, bimodal, or any combination of these in a narrow or broad format. The challenge would now be its application in the industry regarding the difficulty of bubble sampling. In addition, issues with imaging and photography methods would surface in individual bubble discrimination, shape identification, resolution, required quantity of images to represent statistical values. The developed UCT analyzer also came with its setbacks in reproducing the BSD. Nonetheless, new methods have sprung up, curtailing most of the limitations previously mentioned, making it suitable enough to make sound engineering decisions. A classic innovative and industrially accepted example is the McGill Bubble viewer shown in Figure 2.7, with its in-house built bubble size analyzing software (Nesset, 2011).

The measurement comprises three steps: image collection, image processing, and data analysis. First, bubbles are harnessed via a sampling tube into the viewing section, prefilled with water or frother solution, exposing them under pre-set lighting conditions to be imaged. The images are acquired by photographing the bubbles against backlighting as they glide up a 15° sloped window. This window distributes the bubbles into a near monolayer, producing both an unambiguous plane of focus and reducing bubble overlay and 'ghost' images of bubbles in the background. A magnification of usually 25 pixels/mm in plant work, a frequency of about 500 every two seconds, and image number are essential parameters noted during image collection.

A bubble sizing software developed at McGill automatically handles all the images captured in a single experiment for image processing. During image processing, the selection of threshold (maximum grayscale intensity value of a pixel to discriminate objects from background), and up to six bubble selection criteria (for instance, minimum minor and major axes size, aspect ratio range, and shape factor) are required to establish that objects are bubbles. Processing begins with the creation of a binary image when pixel intensities are compared to the threshold; that is, pixels with values below or equal to the threshold are given a value of 1, whereas those with higher values are given a value of 0. Groups of adjacent '1' pixels are considered objects. Objects that are accepted as bubbles are those that meet all selection criteria. The program retrieves the data and arranges the bubbles into frequency distributions based on the equivalent diameter of a circle with the same area as that exposed in the image. Cumulative size distributions and frequency are displayed in plots with both linear and logarithmic size scales, and average diameters such as D_{32} or D_{10} are determined (Gomez and Finch, 2007).

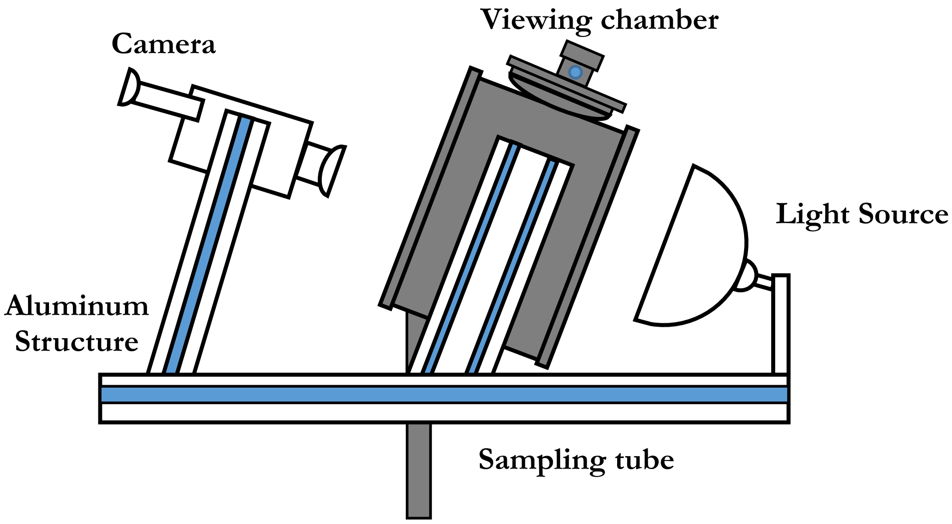

Figure 2.7: Diagram showing the parts of a bubble viewer. Modified from Gomes and Finch, (2007).

2.6 The role of CCCs on bubble size

The concept of Critical Coalescence Concentration (CCC) was first introduced by Cho and Laskowski (2002) to define the concentration beyond which there would be no further bubble coalescence (Sovechles and Waters, 2015). With increasing frother concentration, bubble coalescence is prevented, thereby reducing bubble size to a point where there is no further reduction, as seen in Figure 2.8. At that point, the CCC is reached, and with a further increase in frother concentration, no changes to bubble size would occur (Cho and Laskowski, 2002; Chipfunu *et al.,* 2019). The CCC phenomenon is an indication of bubble size reduction (Zhou *et al.,* 2016).

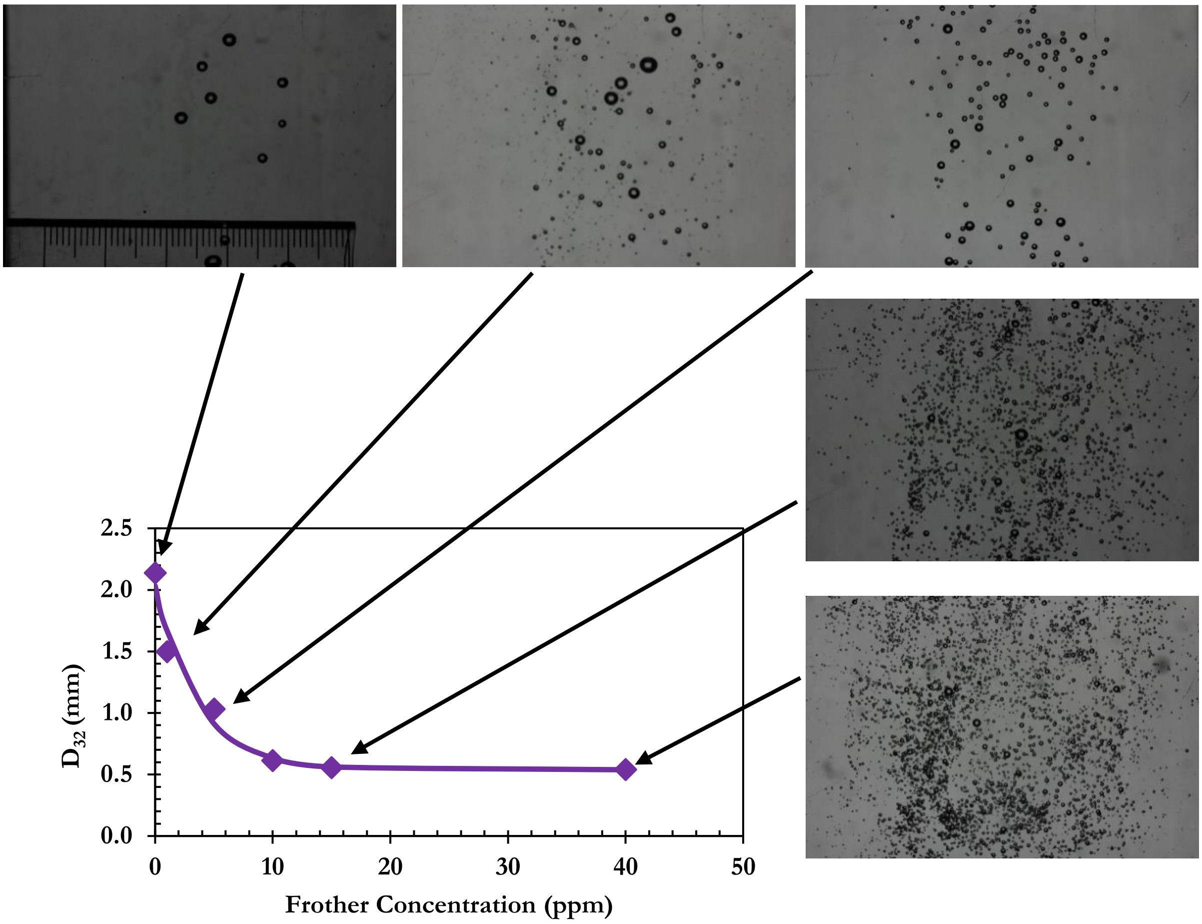

Figure 2.8: Diagram showing the effect of increasing frother concentration/dosage with decreasing bubble size[2].

The Sauter mean diameter (D_{32}) is thus calculated from the measured bubble size distribution (BSD) and thereafter, plotted as a function of frother concentration (C). The resulting D_{32}-C curve drawn shows a sharp initial decrease in D_{32} and plateaus at a point. The curve is divided into two zones (Shown in Figure 2.9) which depict the capability of the solute to prevent bubble coalescence in Zone I, while Zone II shows the bubble break-up mechanics aspect. D_l (limiting bubble size) is a property used to describe the latter phenomena. The point of interception of the two zones is defined as the CCC (Cho and Laskowski, 2002).

---

[2] This work
Frother: MIBC
Air rate: 1.5cm/s

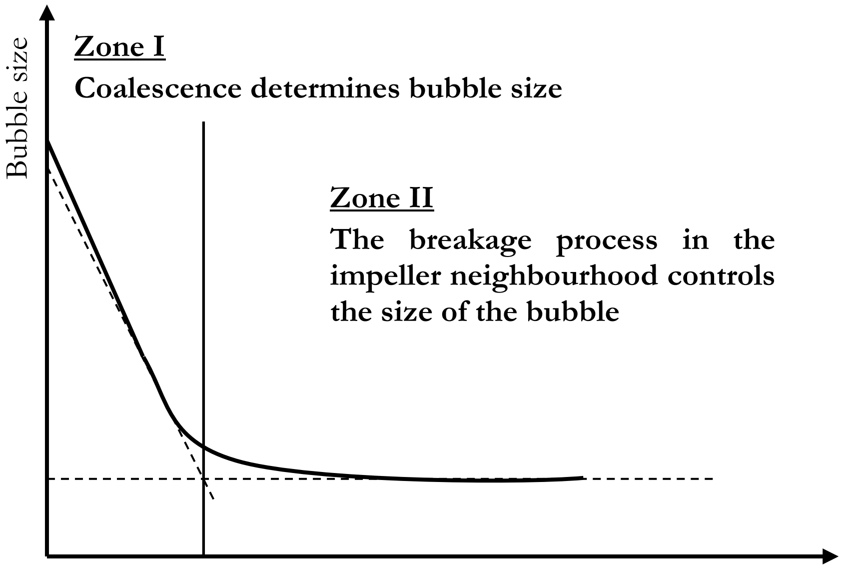

Figure 2.9: Illustration of the effect of solute concentration on bubble size in a flotation cell. Adapted from Cho and Laskowski (2002).

The difficulty with extracting the CCC value for a given frother from experimental data is pinpointing the precise location of the CCC from an exponentially limiting curve. Laskowski provided a graphical method that intersects two lines tangent to the upper and lower portions of the bubble size vs. concentration curve. Still, the technique is somewhat impractical and does not lend itself to mathematical analysis. The notion of CCC_{95} was therefore introduced by Nesset *et al.* (2007), adapting the exponential decay equation of Hernandez-Aguilar *et al.* (2005), defining the concentration for which the bubble size has been reduced to within 5% (i.e., 95% reduction) of its limiting value. This approach is mathematically straightforward and has been extended to define other levels of frother concentration relative to the CCC, generically referred to as CCC_X, such as CCC_{75}, CCC_{50}, and CCC_{150} (representing 2X the CCC_{75} concentration) as depicted in Figure 2.10. Nesset (2011) proposed a 3-parameter model to fit the $D_{32} - C$ data shown in Equation 2.8.

$$D_{32} = D_l + Aexp[-B * C] \tag{2.8}$$

Where D_l (mm) is the limiting D_{32} as the concentration tends to infinity, A (mm) is the change in bubble size between infinite frother and zero frother concentration, B (ppm^{-1}) is the decay constant, and C (ppm) is the solute concentration.

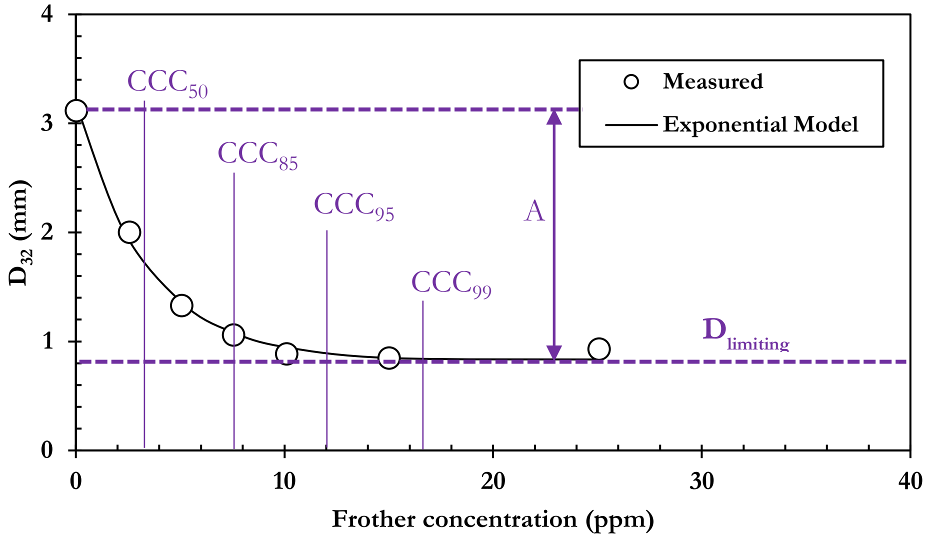

Figure 2.10: Depicting the exponential model used to fit the D_{32} - C data. The CCC_X lines indicate the solute concentration levels for X % reduction in A. Adapted from Nesset (2011).

The CCC for a specific frother shows the concentration required to produce minimum bubble size and maximum S_b. In addition, the shape of the curve that describes the relationship between froth creation and bubble size reduction at various concentrations is different for each frother type. Since frothers work in the aqueous phase, their addition to the circuit should be determined by the ppm concentration in the water phase rather than the metal value or g/t of ore in the circuit feed. As stated, the g/t (ore or metal basis) of frother is related to the ppm by the % water of the pulp, thereby making the actual ppm in solution a posteriori calculation, instead of the desired set point, as the tonnage and ratio and tonnage of water to solids may vary (Cappuccitti and Nesset, 2009).

The addition of sufficient frother at a given air rate to produce minimum bubble sizes results in a maximum bubble surface area flux (S_b), thereby increasing flotation kinetics. For this reason, the concentration within the pulp should always be set close to the CCC of the frother unless other targets are required. In a case where J_g varies towards down a bank of flotation cells, an important observation is that optimum frother concentration increases with air rate (Cappuccitti and Nesset, 2009). Therefore, stage addition is essential to consider in order to maintain the frother at the required CCC at each stage, as the frother may concentrate into the froth phase, evaporate with air from the cell or deplete within the pulp descending the banks. Volatile frothers like alcohols such as (MIBC) are more susceptible to depletion than glycol-based products. An increase in bubble size, loss of flotation kinetics, and, consequently, decreased mineral recovery would result from failure to sustain the optimum frother concentration, mainly where the circuit is composed of more complex mineral components being recovered. In plants where weak frothers are used, they proactively add more frother, exceeding the CCC to prevent the frother concentration from falling below CCC as the conditions change downstream (Cappuccitti and Nesset, 2009).

2.7 Frother characterization

The type of frother significantly impacts parameters such as Sauter mean bubble diameter (D_{32}), water-carrying rate, and gas holdup (ε_g). Frother strength is characterized by several methods based on the aforementioned parameters. Therefore, a strong frother is described as notably possessing a smaller bubble size, a high gas holdup, and a higher water-carrying rate. However, an increased frother strength leads to a less selective mineral recovery. (Zhou *et al.*, 2016). Amongst those who pioneered research into characterizing frothers, Laskowski (2003) attempted to capture both roles in characterizing frothers to provide a basis for selecting frothers for a specified purpose and delved into the connection between frother chemistry/structure and function (Cappuccitti and Nesset, 2009). CCC is also a parameter in the characterization of frothers (Chipfunu *et al.*, 2019).

Frother selection for a targeted purpose is deemed majorly empirical. However, progress is still being made in developing tests to characterize frothers to aid in frother selection (Tan *et al.*, 2018). Currently, several tests are still being developed to aid in the selection and characterization of frothers, as the processes that exist are empirical. Through the process of choosing frothers, most of these tests are conducted by using the bubble column; however, connecting frother functions to frother structure which accelerates the attainment of a frother with ideal or specific properties, is much desired (Kowalczuk, 2013; Finch and Zhang, 2014; Corin and O'Connor, 2014; Wills and Finch, 2016).

The characterization tests that are available include the use of froth half-life, which shows the time needed for the froth to decay to half its initial height once the air is turned off. In addition, frother candidates are screened by using froth height versus GH in water-air experiments (Cappuccitti and Finch, 2008). Characterization tests are formulated to express both functions, namely: the froth stability function, with the estimation of the equilibrium froth height and determination of bubble rise velocity and size (air dispersion), as well as pulp related functions (Zhang *et al.,* 2013; Wills and Finch, 2016).

The blend of polyglycol and alcohol frothers has been used to characterize air dispersion and froth stability. The interaction between the two blends impacted froth properties, where the froth height in the blend was more significant than the sum of individual frother's froth heights (Tan *et al*., 2005). Elmahdy and Finch (2013) reported a synergistic effect on froth height using a blend of polyglycol and alcohol frothers. However, they found that bubble size increased with a small addition of polyglycol to the alcohol above its CCC.

Other developed characterization techniques include frother analysis, which comprises colorimetry, gas chromatography, calibrations of bubble size and gas holdup versus frother concentration, and total organic carbon (Zhang *et al*., 2013). An application of these characterization methods is in determining the ability of the frother to distribute between the froth and the pulp (Gélinas and Finch, 2007).

Measuring frother directly can also be used to assess frother recycled in reclaimed process water or remaining levels in several other effluent streams (Gélinas and Finch, 2007). Frother analysis-procedure and plant experiences measuring frother directly aid process plants in identifying the quantity and location of frother addition to enable proper optimization of the process.

2.8 Effect of Temperature on Flotation

Flotation is an incredibly complex process involving several phases and depends on several operational parameters. An example of an operating parameter affecting the metallurgical performance of a flotation process is the pulp temperature (Drzymala *et al.*, 2022). Bailey and Whelan (1957) studied the effect of temperature on coal flotation. They compared the flotation performance of two types of coal: Penalta (easily floating) and Bedlington E (slow floating). The results showed that the optimum temperature in terms of yield was in the range of 20-30 °C. In addition, they found out that coal yield fell from 72% to 65% for Penalta coal at 25 °C and 10 °C, respectively. Compared to Bedlington E coal, the yield fell from 77% to 22%. Overall, flotation performance deteriorated below 20 °C. The authors attributed the results to changes in the viscosity of the pulp.

Lazarov *et al.* (1994) studied the effect of temperature flotation kinetics of quartz. Flotation tests were conducted in a 0.5 L, operating at 2500 rpm flotation. The temperature varied from 20-40 °C. Dodecylamine hydrochloride (DDAHCL) was used as a collector, and the results were presented for the 90-160 μm size class. The results showed that an improvement in flotation recovery was observed at elevated temperatures for small particles of quartz. Conversely, recovery decreased for larger particles when the temperature dropped.

Investigating the influence of temperature on carbonaceous flotation, Bhattacharya *et al.* (2002) carried out coal flotation in a 2.5 L Agitair flotation cell operating at 750 rpm in batch mode. Diesel oil and synthetic frother were used as flotation reagents. Their result is presented in Figure 2.11. As can be seen, coal yield, flotation rate, and combustible recovery improved with a rise in temperature. They attributed the results to a reduction in the reagents' viscosity and frother and water surface tension at elevated temperatures.

O'Connor *et al.* (1984) studied the effect of temperature on the flotation of pyrite. Flotation tests were carried out in Leeds flotation cell using sodium mercaptobenzothiazole (SMBT) and triethoybutane (TEB) as collector and frother respectively. The effect of temperature on pyrite recovery from their results is depicted in Figure 2.12. Their results show that provided flotation is performed at extended times, not much difference can be observed in the recoveries with temperature changes. The inadequate recoveries at lower temperatures were compensated using longer residence times.

Furthermore, the flotation rate of pyrite exhibited a marked decrease and poorer grades below 10 °C. They attributed the poor performance at low temperatures to a reduction in the rate of mass transfer of pyrite from the pulp to the froth zone. They opined that viscosity increases at low temperatures resulting in a slower rise of bubbles and not due to fewer bubbles per unit volume. Bubble size, however, was not measured in the study.

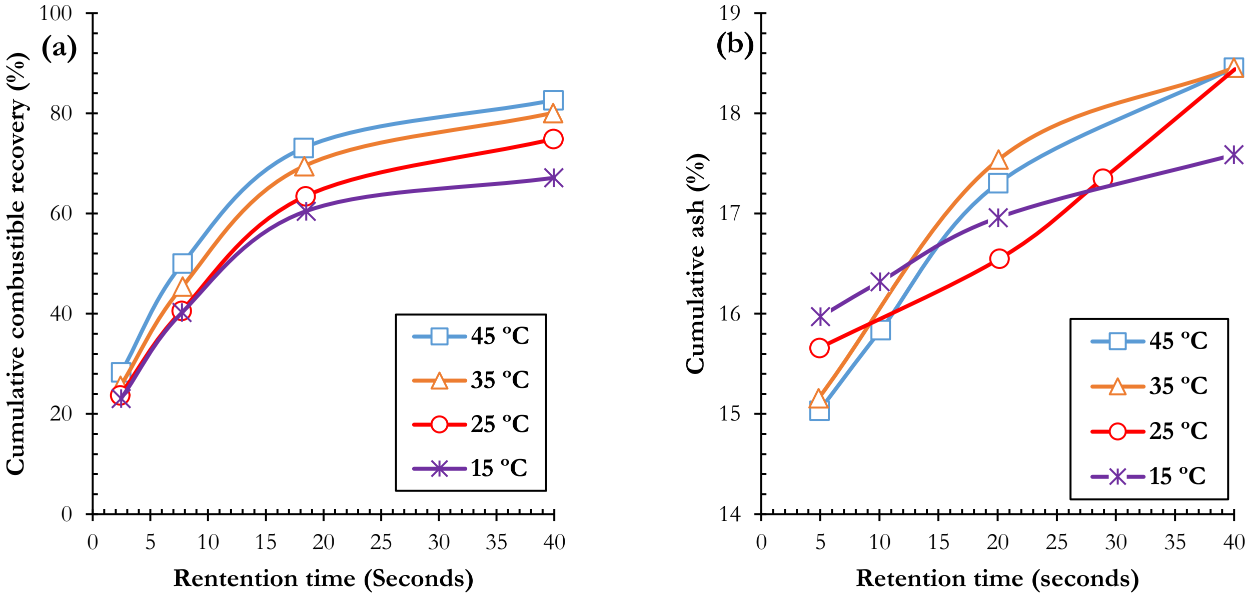

Figure 2.11: Effect of retention time on (a) cumulative recovery, (b) cumulative ash of coal. Modified from Bhattacharya *et al.* (2002).

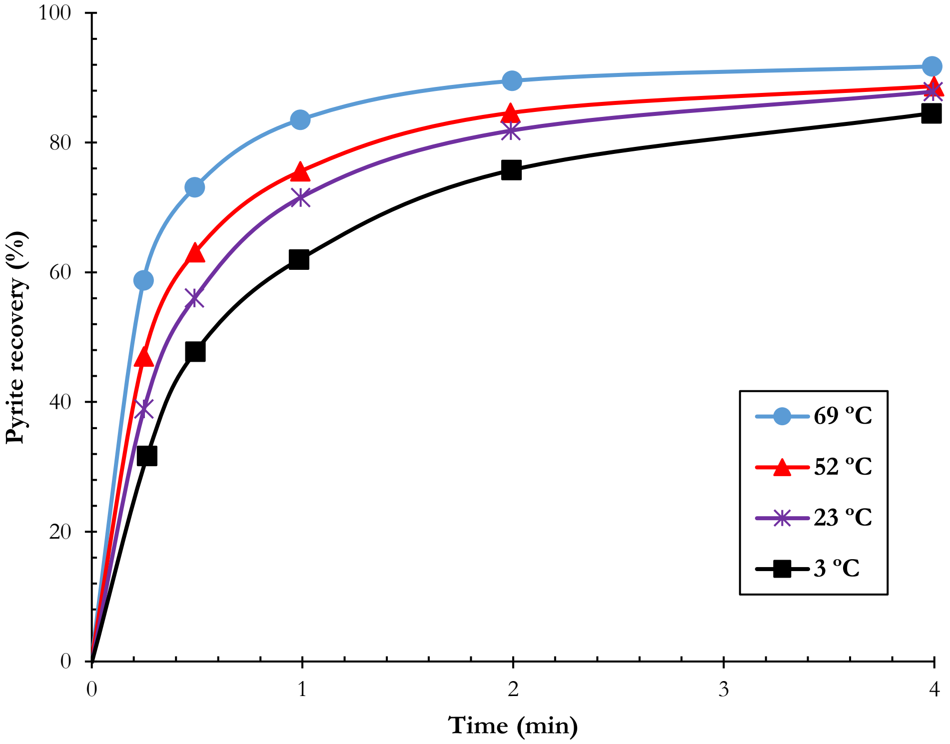

Figure 2.12: Effect of temperature on pyrite recovery. Modified from O'Connor *et al.* (1984).

Klassen (1963) studied coal flotation in continuous operating plants at high temperatures. He reported good concentrate recoveries between the temperature range of 20-30 °C. The adverse effects of flotation at low temperatures or below 10 °C were ameliorated by increasing frother dosages and conditioning times. Bhattacharya and Pascoe (2004) reported similar flotation behavior, indicating improved flotation performance at a temperature range of 20-35 °C.

2.9 Effect of Temperature on frothing/froth stability

Froth structure and stability play an important role in the metallurgical performance of flotation operations. The ability of bubbles in the froth to resist bubble coalescence and bursting is known as froth stability (Farrokhpay, 2011). The effect of temperature on frothing properties and froth stability has been well documented. The effect of temperature on the frothing properties of pine oil (a non-polar frother) was studied by Sun (1952). He found out that the volume of froth produced increases with the temperature of the liquid. Conversely, the amount of aeration required for an increase in froth decreased with an increase in temperature, as seen in Figure 2.13

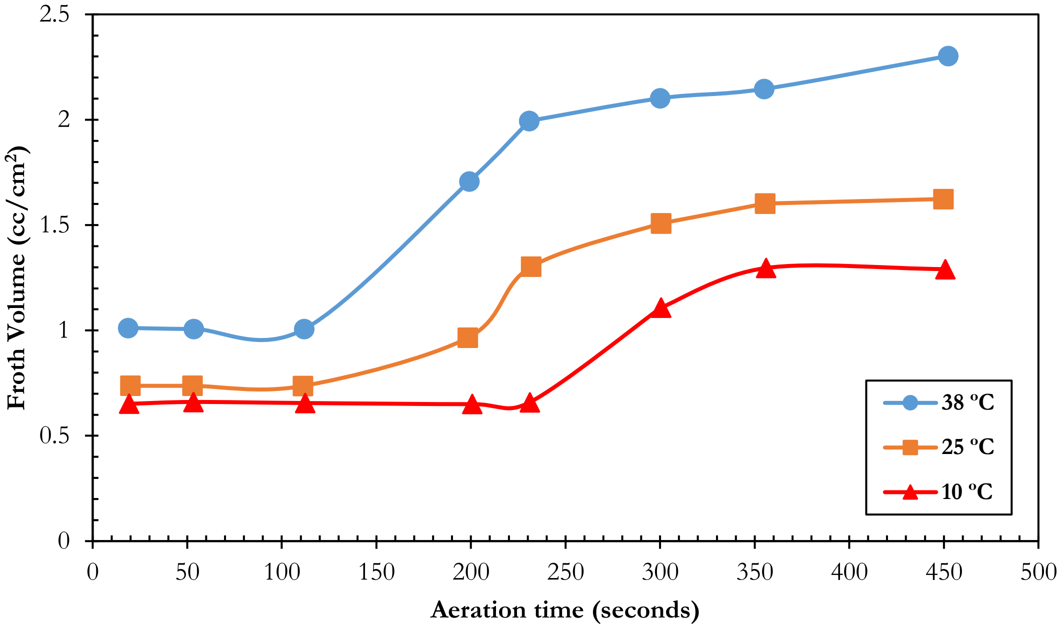

Figure 2.13: Effect of solution temperature on the frothing properties of pine oil. Modified from Sun (1952).

The studies by Sun (1952) indicate that high viscosity, solubility, and increased surface tension of pine oil were observed at low temperatures. Studying the effects of nonpolar reagents on the dispersion of air, Tsiperovich and Sorokin (1964) found that hydrocarbons with different viscosities (note that temperature has an inverse relationship to viscosity) have different frothing influences. Their studies also showed that with a decrease in bubble size, the concentrate recovery increases, and a successful flotation depends on the frothing agent's ability to disperse air. It can be deduced that finer bubbles are produced at higher pulp temperatures (Bhattacharya and Pascoe, 2004).

2.10 Effect of Temperature on bubble size

Plant operating conditions can vary widely in particle size, solid content, and pulp temperature, ranging from 0 °C and 70 °C, which affects the viscosity of the pulp. According to Nesset (2011), the subsequential temperature effect on bubble size is important to numerous flotation plants that experience seasonal changes, as much as a change in 35 °C in Canadian plants. This drastic temperature change has been a primary concern to plants due to the significant drop in recovery during the colder months, then a substantial increase in recovery in the hotter periods. However, the impact of testing viscosity changes directly on bubble size, as much as decreasing particle size or increasing solids concentration, is not known. Furthermore, to the author's knowledge, not much work has been done linking pulp temperature to bubble size. The closest research found online was by Zhang (2014), who delved into the effect of viscosity on bubble size to investigate the impact of seasonal variations on pulp viscosity, water temperature, and, subsequently, bubble size.

Thus, in the studies by Zhang (2014), solids were neglected to focus specifically on the viscosity effect from changes in water temperature akin to seasonal changes. The temperature effect on bubble size in flotation was measured to attain the viscosity effect. A pilot plant experiment was conducted using an RCS^{TM} 0.8 m^3 Metso cell. A McGill bubble size analyzer was used to capture the bubbles to determine the Sauter mean diameter (D_{32}). This result is presented in Figure 2.14.

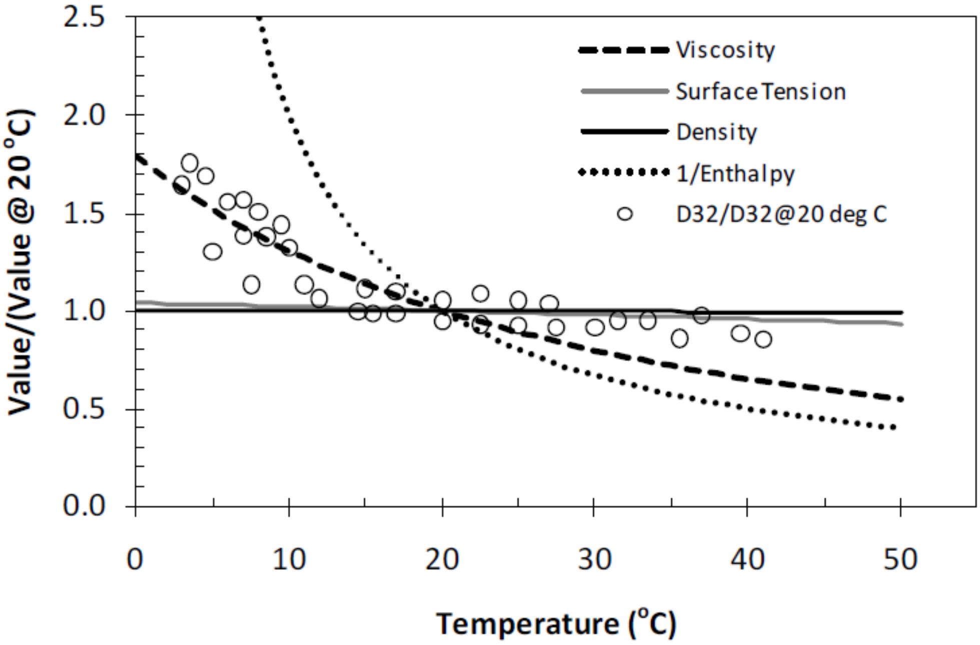

Figure 2.14: Relative values of density of water, surface tension, viscosity, and inverse enthalpy to their values at 20 ^{O}C as a function of temperature (Nesset, 2011).

It was established that viscosity significantly impacted bubble size, and other properties of water that are temperature-dependent could also affect bubble size distribution. Consequently, a model was also developed which predicted that water viscosity increases at 5 °C with a corresponding

D_{32} increase of approximately 1.38 mm. As a result, the rate constant decreased to 0.109 min^{-1} and a recovery loss of 2.4%.

Navarra *et al.* (2009) studied the impact of frother on the terminal velocities of small bubbles (< 1mm). In their studies, two common industrial frothing agents, MIBC and Dowfroth 250, were used with temperatures ranging from 20-30 ºC. The results show that for both frothers tested, the terminal velocities were below that of the stokes model. Furthermore, they observed that the addition of frothers retard the bubbles beyond the prediction of the hard sphere model, implying that the motion of small bubbles appears to be impeded by the same mechanism as those acting on larger bubbles.

Studies from existing literature have shown significant work on the effect of temperature on flotation variables. However, no significant work has been done on investigating the effect of temperature on bubble size. Although the work of Zhang (2014) evaluated the effect of viscosity changes by varying water temperature between 3-5 °C, a limitation of his study might be the potential loss of heat during transfers and the inability to maintain the water temperature over the duration of the tests. This thesis would delve specifically into the effect of temperature solely on bubble size using two main frother types, predict its association or impact on bubble surface area flux, and possible connection to recovery. The water temperature would be controlled by employing an Isotemp bath to maintain specific setpoints throughout the tests.

CHAPTER THREE: MATERIALS AND METHODS

3.1 Materials

Reverse osmosis/deionized water from the reverse osmosis tank (Barnstead International, USA, Model D12651) was used in this experiment. The water was collected during the summer period to maintain a constant average temperature of 21 °C. For each superficial gas velocity, temperature, and concentration setpoint for a specific test batch, water was collected and stored to ensure consistency in test results without much change in chemistry for the identical test batches. The frothers used in this study are summarized in Table 3.1.

Table 3.1: Specification of frothers

Frother family	Chemical Structure	Commercial type	Supplier	Molecular weight
Aliphatic Alcohols	$C_nH_{2n+1}OH$	MIBC	Sigma Aldrich	102g/ mol
Polypropylene glycol	$H(OC_3H_6)_mOH$	PPG 425	Sigma Aldrich	425g/ mol

Table 3.2: Camera type and model

	CANON EOS 60 D	CANON 90 D
Continuous shooting	5 fps	11 fps
Battery life	1100 shoots	1300 shots
Number of focus points	9	45
Megapixels	18	33 megapixels
Max mechanical shutter	1/8000s	1/8000s
Max video resolution	1920 x 1080	3840 x 2160
Dimensions	145 x 106 x 79 mm	141 x 105 x 77 mm
Lenses	Canon EF/EF-S	Canon EF/EF-S

Canon 60 D and Canon 90 D cameras were used to capture bubble sizes to attain high resolution. A 2-sigma canon macros 70 mm focal length lens was used: The specification of the camera model is shown in Table 3.2.

3.2 Methods

This work involved finding a suitable methodology to determine the changes in the Sauter mean bubble diameter, representing the bubble size in a mechanical cell, by varying the temperature of the pulp at different setpoints between a range of 5 °C and 40 °C. The methodology involved two processes: altering bubble size by varying temperature in the mechanical cell and analyzing the bubbles to determine the Sauter mean diameter (D_{32}) of the bubbles. The temperature ranges selected for all the parameters were representative of industrial practice. The pulp primarily consisted of a frother solution (liquid-air phase system). The two-phase system was considered in this research to ensure the temperature effect on bubble size in the liquid phase without the interference of solids.

As shown in Figure 3.1, temperature measurement was achieved using the Isotemp bath circulator (Fischer Scientific, USA, Model 4100 R20). The Isotemp bath circulator is a heat and cold exchange system, so a cooled or heated ethylene glycol is transferred from the bath to the bucket containing frother solution to control the temperature of the solution within the bucket. For each temperature setpoint, the Isotemp bath circulator was set at a higher setpoint to attain the frother solution's desired temperature. This method was employed due to the differences in the thermal properties of ethylene glycol and the frother solution. The frothers used for these experiments were PPG 425 and MIBC to establish the effect of both frother types.

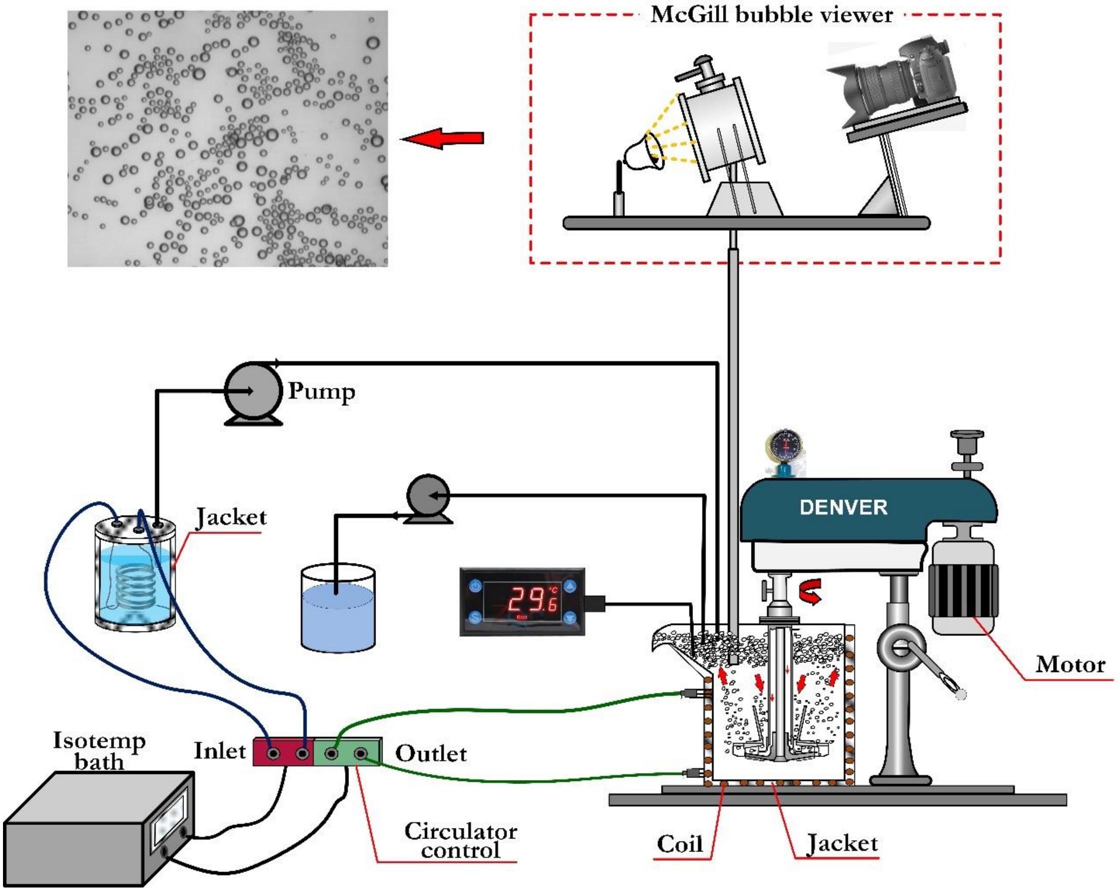

Figure 3.1: Overview of the setup showing the process of varying temperature effect on bubble size.

The CCC_{95} for each frother type was determined at a given superficial gas velocity. For each test, the desired frother was added in their respective concentrations into a bucket containing 10.7 L of deionized water. Deionized water was used in all the experiments to eliminate the ionic effect on bubble size in this process. Once the frother solution reached the desired temperature, the solution was pumped into the Denver mechanical cell. Next, the impeller was turned on, and compressed air (superficial gas velocity) was introduced into the cell. The impeller induces turbulence, thereby generating bubbles within the system. The next stage involved harnessing the bubbles from the cell through a sampling tube to be captured in the bubble viewing chamber. The measurement comprises three steps: image collection, image processing, and data analysis. Bubbles were harnessed via a sampling tube into the viewing section, filled with water or frother solution, exposing them under pre-set lighting conditions to be imaged. The sampling tube, situated above the Denver cell, connects the bubble viewing chamber to the bubble generation zone within the mechanical cell. The images were then acquired by photographing the bubbles against backlighting as they glided up a 15-degree sloped window. Thereafter, the bubble sizes were captured by using a canon 60 D, and an inbuilt McGill bubble size analyzer was used to determine the Sauter mean bubble diameter (D_{32}) from the captured bubble images. It should be noted that the analyzed images contained a minimum of 10,000 bubbles to ensure a large data set for single tests and statistically significant results (Sovechles *et al.,* 2016). For each temperature setpoint, five tests were conducted to ensure repeatability and reproducibility.

CHAPTER FOUR: RESULTS AND DISCUSSION

This section presents and discusses the following results in subsections: The determination of CCC_{95} at different gas rates (J_g) of 0.5 cm/s, 1 cm/s, and 1.5 cm/s for both MIBC and PPG 425 frothers in order to measure the CCC for subsequent temperature tests; determining the CCC_{95} with changes in temperatures or the determination of CCC_{95} with changing temperatures; and confirmatory tests of temperature effect on bubble size (D_{32}) at measured CCC_{50} and CCC_{95}.

As indicated in section 3.2, tests were conducted in a Denver flotation cell using two commercially used frothers, MIBC and Polyglycol (PPG 425). The aim was to investigate the effects of the various parameters (gas rates, concentration, and temperature) on the two different frother types representing two contrasting chemistries and structures.

4.1 Determination of CCC_{95} at different gas rates

The results of these experiments are shown in Figures 4.1 and 4.2. The Sauter mean diameter (D_{32}) was plotted as a function of frother concentration to determine the critical coalescence concentration and its corresponding D_{32}; for a concentration range of 0-40 ppm and gas rate of 0.5-1.5 cm/s. The water temperature was maintained at room temperature (21 ± 1 °C), both for MIBC and PPG 425. The experiments were conducted to ascertain specific setpoints, eliminate guesses, and be consistent with industry parameters.

The Nesset model (Equation 2.8) was fit to the data. In addition, the CCC_X for CCC_{95}, as well as their corresponding $D_{32,}$ were calculated using the formulas below (Quinn *et al.,* 2014):

$$CCCX = -\frac{In(1-X)}{B} \tag{4.1}$$

$$D_{32} = \frac{\sum d_b^3}{\sum d_b^2} \tag{4.2}$$

For D_{32} versus concentration at the aforementioned setpoints, the trends, as seen in Figures 4.1 and 4.2, show an exponential decay curve exhibiting a limiting bubble size, that is, D_l, with increasing concentration which is likened to ppm approaching infinity (Equation 2.8). The CCC_X values indicate where the D_{32} values have been reduced to the stated X % in all cases of their respective limiting values. Each curve reveals two regions or sections in all cases: a steep linear portion/slope at lower concentrations and a horizontal, almost constant slope at higher frother concentrations (Grau *et al.*, 2005). This trend is observed in all the plots in Figures 4.1 and 4.2, indicating that with increasing frother concentration, bubble size decreases to a point where there is no further decrease in bubble size (D_l). This concentration point where no further reduction in bubble size occurs is termed the critical coalescence concentration CCC (Laskowski, 2003; Gupta *et al.*, 2007). For both frother types tested, it is evident that there are distinct differences in CCC_{95}. MIBC has higher CCC_{95} than PPG 425, as shown in Tables 4.1 and 4.2. The results indicate that the PPG frother requires a lower concentration to produce the minimum D_{32} or bubble sizes than MIBC, indicating strong frothing properties (Tan *et al.*, 2005; Will and Finch, 2016).

The calculated D_{32} or average bubble sizes recorded at different gas rates for MIBC, and PPG 425 did not vary significantly as shown in Tables 4.1 and 4.2. However, differences in CCC_{95} showed slight differences, which is more prominent in PPG 425. In the case of PPG 425, there was an increase in CCC_{95} from approximately 5.19 ppm to 9.14 ppm as the gas rate was changed from 0.5 cm/s to 1 cm/s, without a significant change in average bubble sizes, calculated from the CCC values, which is consistent with results from Sovechles *et al.* (2016). Similar CCC values for alcohol and polyglycol frothers were reported by Nesset (2011) between 0.5-1.0 cm/s. However, the case seems to be different in the case of 1.5 cm/s, where a decrease in CCC_{95} can be observed. This could be attributed to the higher value of the decay constant B in Tables 4.1 and 4.2. The decay constant for PPG 425 is higher than MIBC for all gas rates tested, typical for frothers with higher molecular weight (Nesset, 2011). Thus, it is plausible that the CCC was attained faster and thereafter remains constant due to a higher gas rate. However, more tests should be performed to ascertain this suspicion or fact. A similar trend can be observed in the case of MIBC, at 1.5 cm/s, somewhat confirming the observation made in the PPG 425 test. Otherwise, this situation could somewhat be attributed to machine effect.

Having established the CCC_{95}, the same setpoints were maintained and calculated for CCC_{50}. The CCC_{50} and D_{32} at 0.5 cm/s for MIBC and PPG 425 were approximately 3.4 ppm and 1.32 mm, and 1.2 ppm and 1.25 mm, respectively for both frothers. Consequently, to determine the effect of temperature on the bubble size of the tested frothers using the calculated CCC_{95} and CCC_{50}, it was first necessary to ascertain whether any significant difference in CCC values occurs at different temperatures.

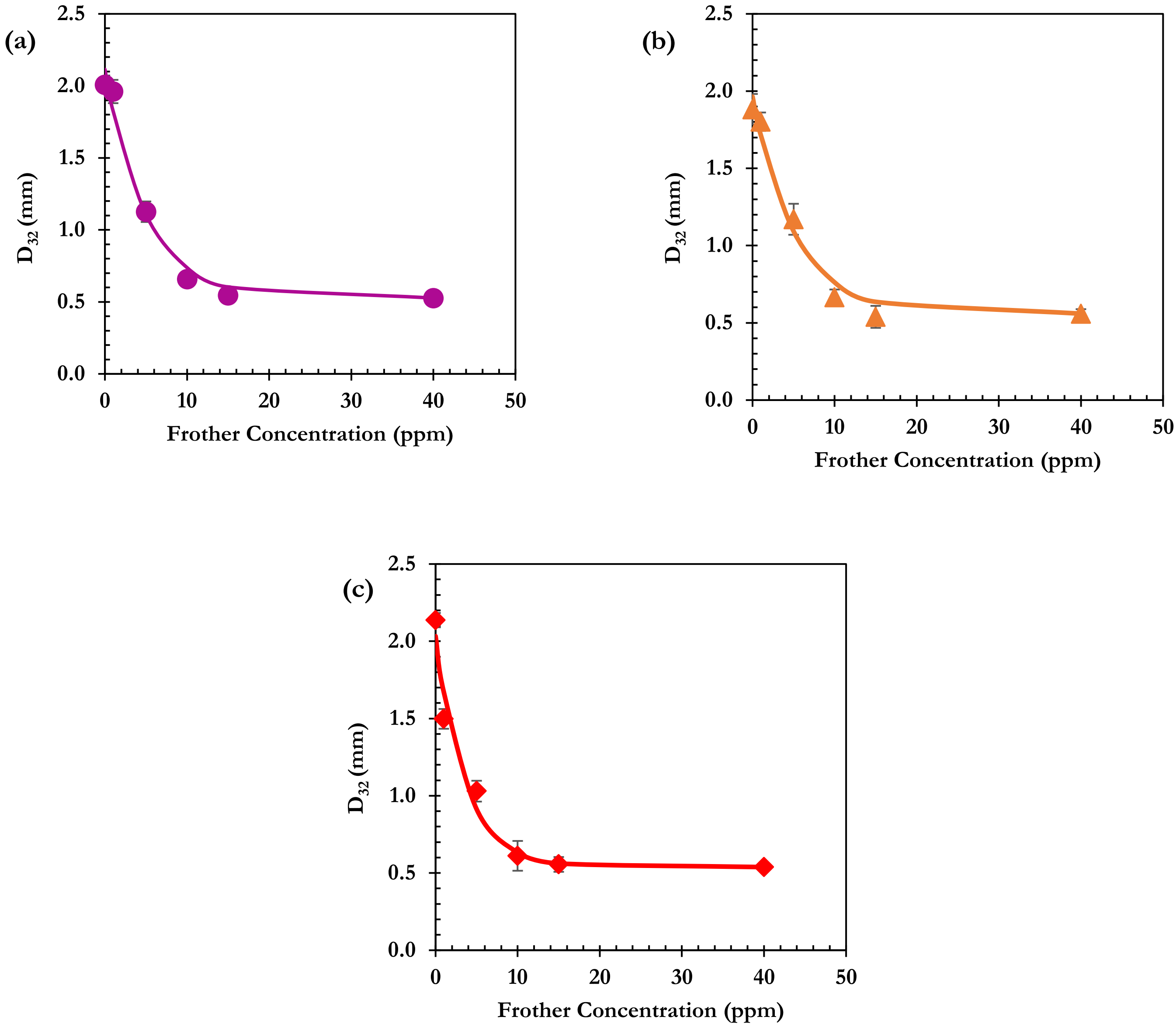

Figure 4.1: Effect of frother concentration (MIBC) on D_{32} at (a) J_g= 0.5 cm/s, (b) J_g= 1.0 cm/s, (c) J_g= 1.5 cm/s. The data points shown are average values with 95% confidence intervals and were fitted with curves generated from the Nesset model.

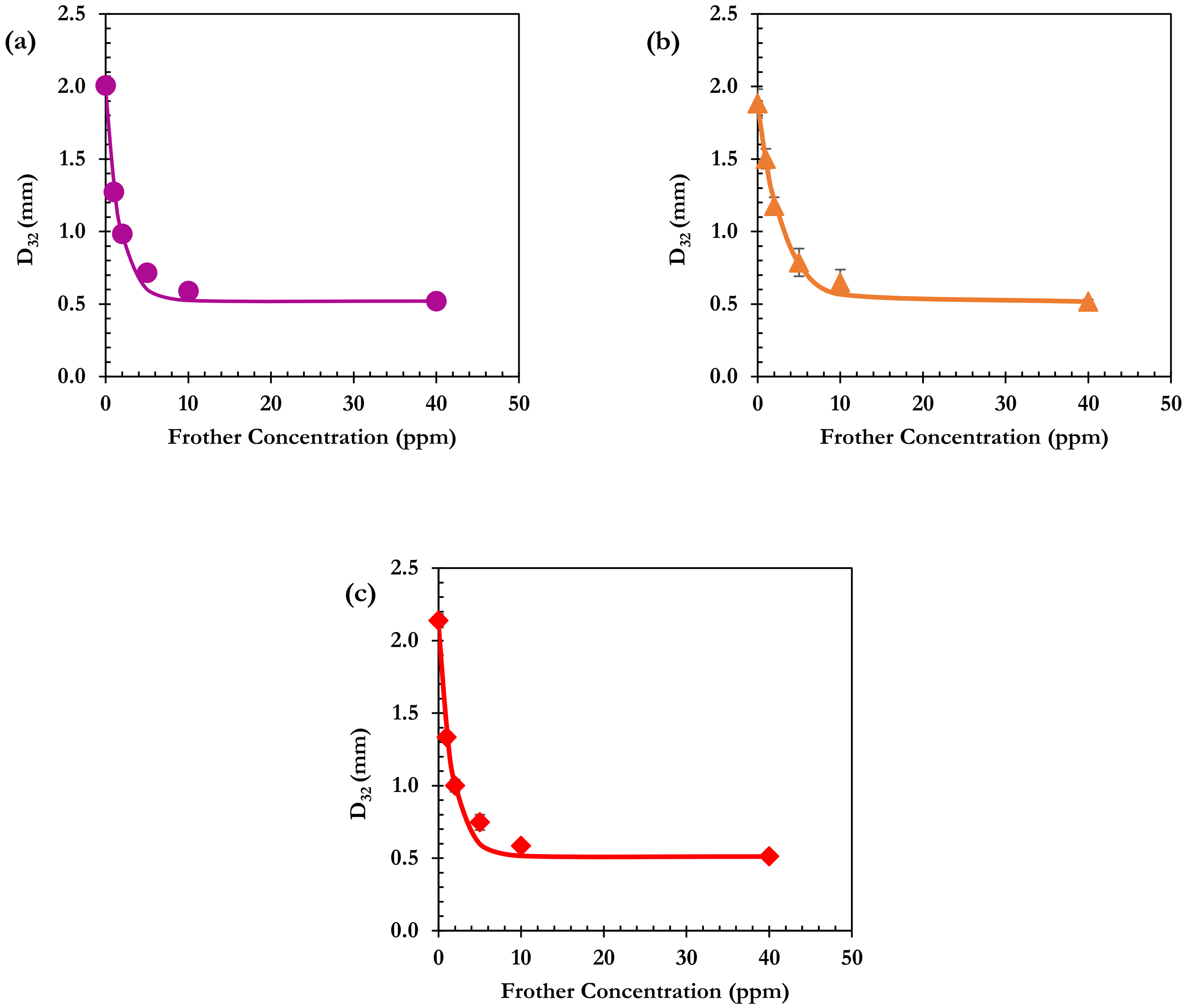

Figure 4.2: Effect of frother concentration (PPG) on D_{32} at (a) J_g= 0.5 cm/s, (b) J_g= 1.0 cm/s, (c) J_g = 1.5 cm/s. The data points shown are average values with 95% confidence intervals and were fitted with curves generated from the Nesset model.

Table 4.1: Model parameters for MIBC concentration with varying gas rates

J_g (cm/s)	D_l (mm)	A (mm)	B (ppm^{-1})	CCC_{95} (ppm)	D_{32} (mm)	R^2
0.5	0.53	1.59	0.20	14.87	0.61	0.98
1	0.56	1.41	0.19	15.48	0.63	0.98
1.5	0.54	1.49	0.28	10.83	0.61	0.97

Table 4.2: Model parameters for PPG 425 concentration with varying gas rates

J_g (cm/s)	D_l (mm)	A (mm)	B (ppm^{-1})	CCC_{95} (ppm)	D_{32} (mm)	R^2
0.5	0.52	1.46	0.58	5.19	0.61	0.99
1	0.52	1.36	0.33	9.14	0.63	0.99
1.5	0.51	1.59	0.58	5.14	0.61	0.98

4.2 Determination of CCC_{95} at different temperatures

Having established the CCC_{95} at the gas rates, the subsequent tests were to ascertain whether there were changes in the CCC_{95} (vis-a-vis D_{32}) with temperature. The same methodology described in section 3.2 was employed for this test. Although, instead of changing superficial gas velocity/gas rate for a given frother concentration range, the temperature was varied (5-40 °C). The temperature was kept constant for each test, with varying concentrations. A gas rate of 0.5 cm/s was maintained, and all other concentration values were maintained for consistency.

Interestingly, the trends witnessed followed the same exponential pattern as discussed in section 4.1. The results and trends for MIBC and PPG 425 are shown below in Figures 4.3 and 4.4 respectively. The figures show a dependency between the Sauter mean diameter and frother concentration.

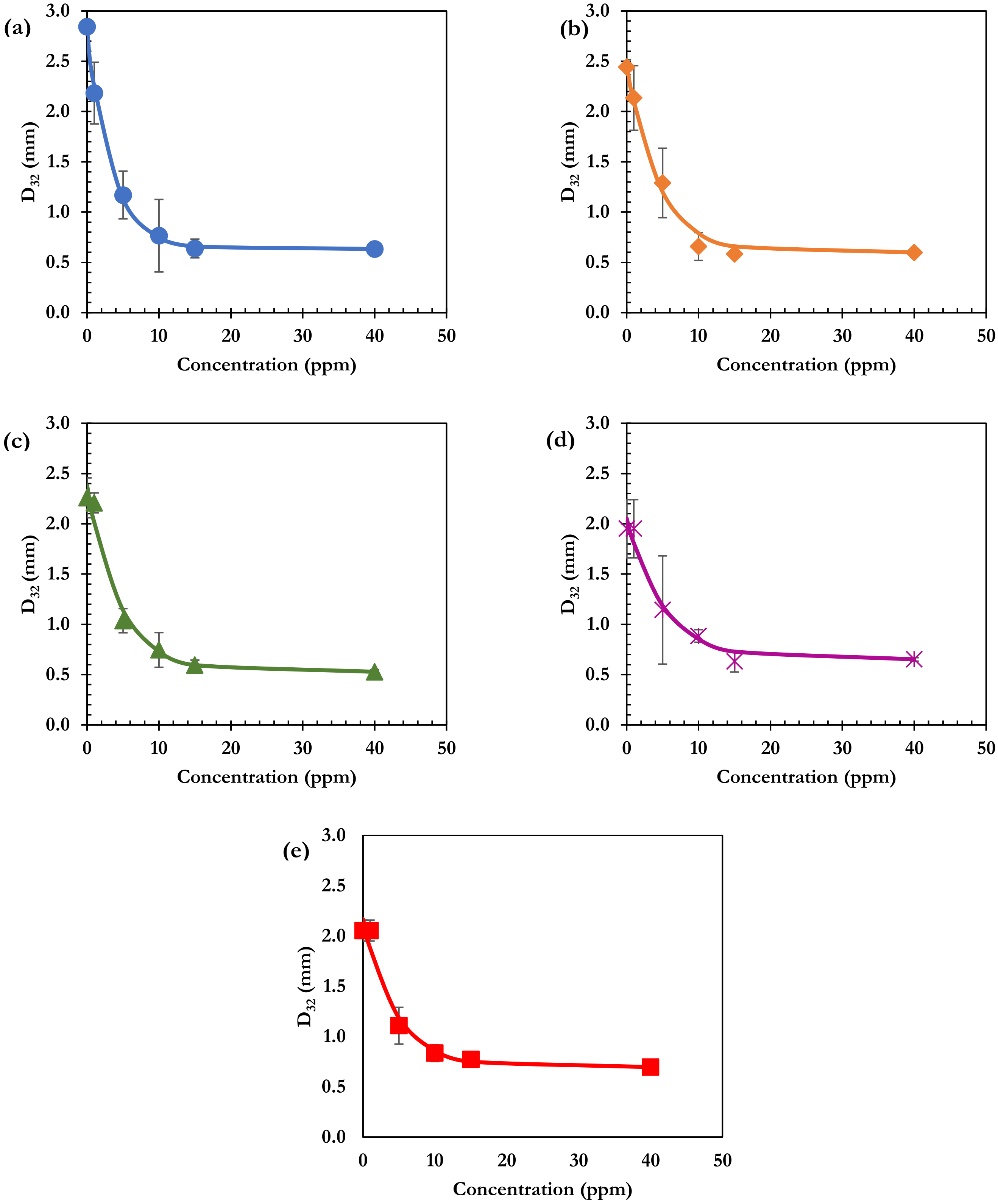

Figure 4.3: Effect of frother concentration (MIBC) on bubble size at (a) 5 °C, (b) 10 °C, (c) 20 °C, (d) 30 °C, (e) 40 °C. The data points shown are average values with 95% confidence intervals and were fitted with curves generated from the Nesset model.

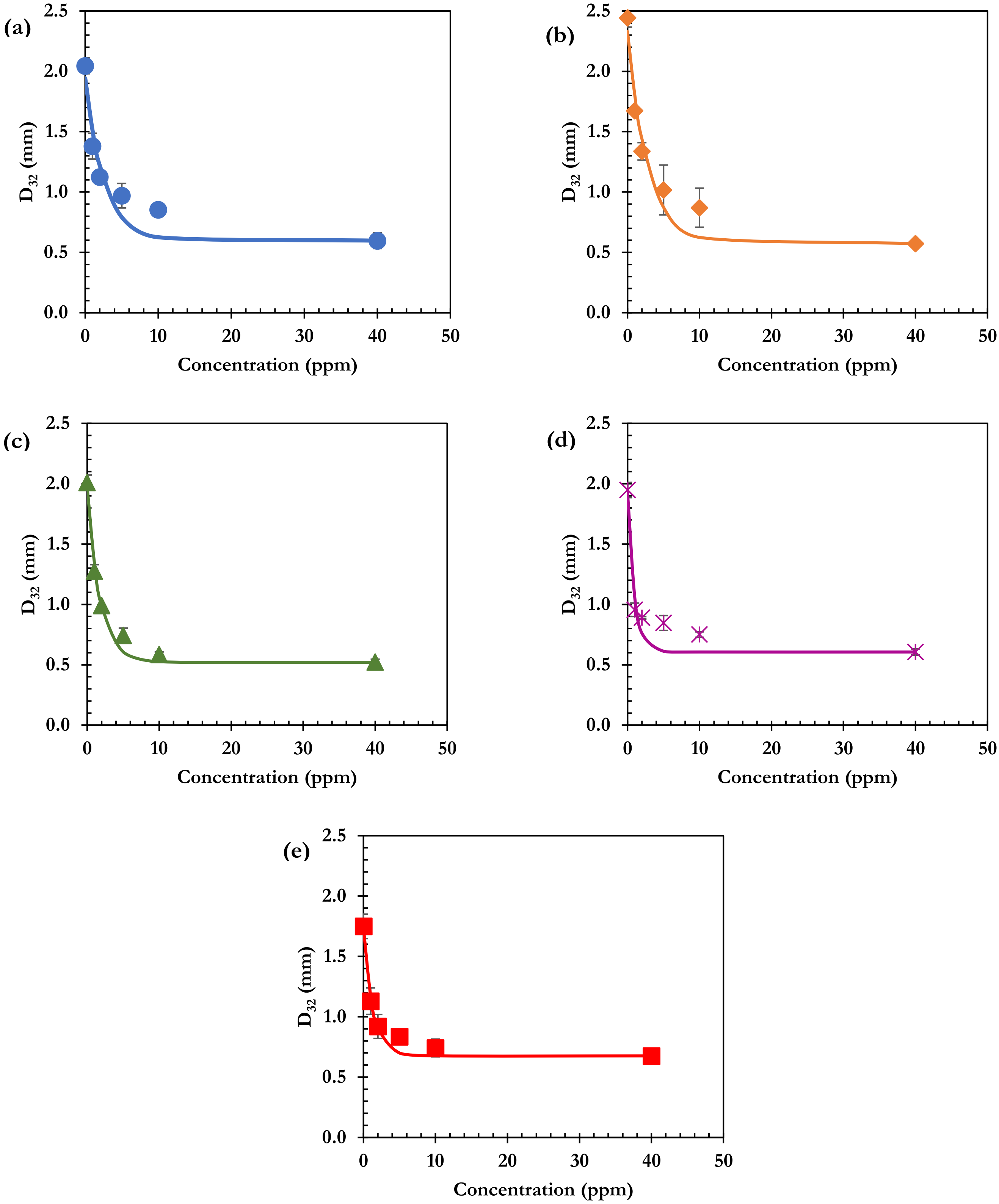

Figure 4.4: Effect of frother concentration (PPG 425) on bubble size at (a) 5 °C, (b) 10 °C, (c) 20 °C, (d) 30 °C, (e) 40 °C. The data points shown are average values with 95% confidence intervals and were fitted with curves generated from the Nesset model.

At each temperature range tested, there was a significant decrease in D_{32} with increasing concentration. As the frother concentration approaches the CCC_{95}, there is seemingly no impact on the average bubble size. Additionally, the Nesset model fit the data well, making results consistent with previously modelled data. A summary of the model parameters (using the Nesset model, Equation 2.8) and measures of goodness of fit is shown in Tables 4.3 and 4.4. The R^2 shows a good correlation with all R^2 values above 0.96 for MIBC and 0.90 for PPG 425. Similar to the results obtained in section 4.1 and as expected, the decay constant (B) was higher for PPG, suggesting a faster rate at which the bubble size decreases with a corresponding decrease in CCC_{95}.

Table 4.3: Model parameters for MIBC concentration with varying temperature

Temperature /°C	D_l (mm)	A (mm)	B (ppm^{-1})	CCC_{95} (ppm)	D_{32} (mm)	R^2
5	0.63	2.17	0.29	10.17	0.74	1.00
10	0.60	1.89	0.23	13.12	0.69	0.99
20	0.53	1.85	0.22	13.53	0.62	0.98
30	0.65	1.40	0.19	15.53	0.72	0.98
40	0.70	1.47	0.22	13.60	0.77	0.97

Table 4.4: Model parameters for PPG 425 concentration with varying temperature

Temperature /°C	D_l (mm)	A (mm)	B (ppm^{-1})	CCC_{95} (ppm)	D_{32} (mm)	R^2
5	0.60	1.35	0.39	7.76	0.66	0.91
10	0.57	1.76	0.35	8.49	0.66	0.95
20	0.52	1.46	0.57	5.30	0.59	0.98
30	0.61	1.32	1.07	2.80	0.67	0.91
40	0.68	1.06	0.76	3.97	0.73	0.97

It can be observed from Tables 4.3 and 4.4 that the CCC_{95} changes with temperature. For MIBC, the CCC_{95} value increased from 10.17 ppm at 5 °C to 15.53 ppm at 30 °C before it decreased. As expected, the CCC_{95} values for PPG 425 were less than that of MIBC for all temperature ranges tested. In addition, the values obtained for PPG 425 at warmer temperatures (20-40 °C) were less compared to colder temperatures (5-10 °C) and vice versa for MIBC. A one-way analysis of variance (ANOVA) was performed to ascertain if there is any significant difference between the mean bubble sizes at different temperatures for a given frother concentration. The ANOVA conducted on the resulting average bubble sizes (D_{32}) shown in Table 4.5 showed a statistically significant difference between the mean bubble sizes at different temperatures for PPG 425 as the *P* values are less than the significance level ($\alpha = 0.05$). To bolster this statement, the F values calculated in the ANOVA tables are more significant than their respective F critical values between the groups compared (mean bubble sizes at different temperatures).

For MIBC, the difference in the means at different temperatures was insignificant at concentrations less than the calculated CCC (see *Section 4.1*), specifically at 1, 5, and 10 ppm (F (4,10) < Fcritical, *P* > .05). However, above 10 ppm, the means differ significantly. It can be observed that the temperature effect on bubble size was pronounced at concentrations at or above the CCC value of MIBC. Table 4.5 shows that temperature has a significant impact on bubble sizes. The obtained results imply that the bubble sizes obtained during summer months could differ from those of winter for the same frother concentration as in the case of PPG 425, shown in Table 4.4.

Table 4.5: ANOVA results on CCC_{95} determination of MIBC and PPG at different temperatures

Frother	Concentration (ppm)	SS	MS	F-value	*P*-value	F critical	Remarks
MIBC	0	1.504	0.376	65.830	3.81E-07	3.478	F (4,10) > Fcritical, *P* < .05
	1	0.132	0.033	3.055	0.069	3.478	**F (4,10) < Fcritical, *P* > .05**
	5	0.104	0.026	1.311	0.330	3.478	**F (4,10) < Fcritical, *P* > .05**
	10	0.082	0.020	2.983	0.073	3.478	**F (4,10) < Fcritical, P > .05**
	15	0.070	0.018	21.864	6.24E-05	3.478	F (4,10) > Fcritical, *P* < .05
	40	0.038	0.010	32.329	1.07E-05	3.478	F (4,10) > Fcritical, *P* < .05
PPG 425	0	0.768	0.192	191.490	2.11E-09	3.478	F (4,10) > Fcritical, *P* < .05
	1	0.880	0.880	188.447	2.28E-09	3.478	F (4,10) > Fcritical, *P* < .05
	2	0.405	0.101	165.231	4.36E-09	3.478	F (4,10) > Fcritical, *P* < .05
	5	0.147	0.037	16.546	2.08E-04	3.478	F (4,10) > Fcritical, *P* < .05
	10	0.158	0.039	32.991	9.80E-06	3.478	F (4,10) > Fcritical, *P* < .05
	40	0.038	0.010	32.329	1.07E-05	3.478	F (4,10) > Fcritical, *P* < .05

4.3 Determination of the effect of temperature on bubble size

The previous section showed that the CCC_{95} changes with temperature. Consequently, the effect of temperature on bubble size was investigated using the frother concentration at CCC_{95} and 0.5 cm/s for both frothers (see *Section 4.1*). The calculated CCC_{95} at 0.5 cm/s was used, since it represents the setpoints used in the mineral processing industry (Nesset, 2011). The effect of temperature on bubble size for both frother types was investigated using the methodology described in section 3.2. Furthermore, reverse osmosis or deionized water was used instead of tap water, as suggested by Zhang (2014), who was one of the first to investigate the effect of viscosity on bubbles by employing temperature variation to delineate the impact of ions/salts found in ordinary tap water. The results are illustrated in Figures 4.5-4.6

Figure 4.5 shows the effect of temperature on bubble size for MIBC. As can be seen, the bubble size decreased from 5 °C to 30 °C. The maximum bubble size was 0.62 mm at 5 °C, while the lowest among the temperature range tested was 0.58 mm at 30 °C. Although polyglycol frothers such as PPG 425 are much more robust and have faster kinetics than alcohols, the differences in bubble sizes between both frothers were marginal above 10 °C. This was expected because, at CCC_{95}, the average bubble size would have been entirely minimized, and frother concentration would have reached saturation. Hence, frother kinetics would appear to be at its maximum. However, below 10 °C, there is a considerable increase in bubble sizes of PPG 425 compared to MIBC. The strong frothing property of PPG 425 is evident in Figure 4.6. It can be observed that there is a marked difference in bubble sizes compared to MIBC above 10 °C. At $CCC_{50,}$ the exponential decay has been reduced by 50% of its limiting value D_l. Thus, PPG 425 showed faster kinetics and approached its limiting values compared to MIBC.

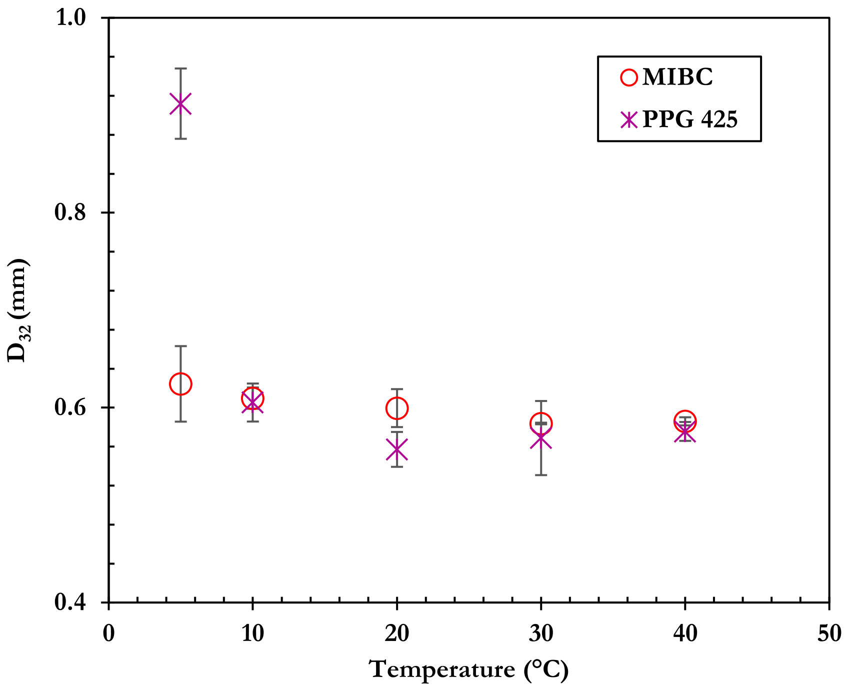

Figure 4.5: Effect temperature on bubble size with CCC_{95} frother concentration. The data points shown are average values with 95% confidence intervals.

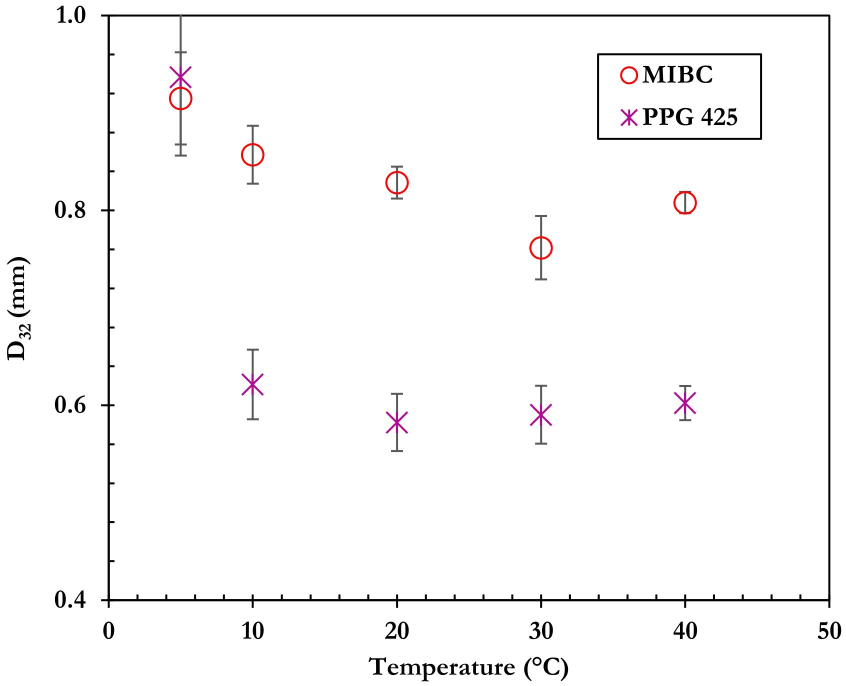

Figure 4.6: Effect temperature on bubble size with CCC_{50} frother concentration. The data points shown are average values with 95% confidence intervals.

Interestingly, the difference between the bubble sizes of PPG 425 at CCC_{50} and MIBC at CCC_{95} is virtually the same. So, it appears that PPG 425 might be advantageous compared to MIBC regarding reagent dosage and frother kinetics (Cappuccitti and Nesset, 2009). However, Figures 4.5 and 4.6 show that these advantages of PPG 425 over MIBC occur only above 10 °C.

Overall, Figures 4.5 and 4.6 show there is an increase in bubble size below 20 °C and above 30 °C. The increase was more evident below 10 °C and for PPG 425. The obtained results are consistent with studies on coal, where concentrate yield and recovery of combustibles appear to be best within the temperature range of 20-35 °C (Bhattacharya *et al.*, 2002; Bhattacharya and Pascoe, 2003). Incidentally, the lowest bubble sizes recorded were within 20-30 °C for MIBC and PPG 425. The efficiency of a flotation process depends on the size of the bubbles as it determines the mass transfer or bubble surface area flux (S_b) from the pulp to the froth zone (Zhang, 2014). Ideally, smaller bubbles are desired as they increase the rate of collision with particles and consequently increase flotation kinetics or mass transfer (Wills and Finch, 2016).

The mass transfer of particles from the pulp zone to the froth zone is affected by temperature (O'Connor *et al.*, 1984). Typically, viscosity increases with a decrease in temperature resulting in a slower rise of bubbles and a reduced rate of mass transfer (Bailey and Whelan, 1958). Therefore, it is plausible that due to the changes in viscosity at lower temperatures, larger bubble sizes are formed, leading to a decrease in the bubble surface area flux or S_b and, thus, a reduction in flotation kinetics or lower mass flux transfer. The data shown in Figures 4.5 and 4.6 suggest that flotation using any of the tested frothers below 10 °C would result in a reduction in the mass transfer or decreased mineral recovery as bubble size increases. Zhang (2014) also reported an increase in viscosity at 5 °C resulting in an increase in D_{32} and a loss in mass transfer for DF 250—a polyglycol frother. The adverse effects of lower temperature on bubble size would be deleterious for flotation and more evident for PPG 425.

CHAPTER FIVE: CONCLUSIONS AND FUTURE WORK

5.1 Conclusions

- A detailed experimental methodology was developed for the determination and measurement of the effect of temperature on bubble size.
- In this study, it was observed that the CCC_{95} for the two industrial frother types (MIBC and Polyglycol-PPG 425) changes with temperature.
- The CCC_{95} values were within the range of 10-15 ppm and 5-9 ppm for MIBC and PPG 425, respectively. It was observed that the CCC_{95} decreased after 1 cm/s for both frothers.
- The study has shown that temperature affects bubble sizes. Above 10 °C, the difference in bubble sizes between both frothers was marginal due to both frothers reaching their saturation at CCC_{95}. However, there was a marked difference in bubble sizes between both frothers at $CCC_{50.}$ PPG showed a significant increase in bubble size below 10 °C, while the lowest bubbles recorded were within 20-30 °C, with an increase observed in lower and higher temperatures within this range.
- The obtained results show that the strong frother properties of PPG 425 over MIBC in reaching its limiting bubble size (D_l) occur only above 10 °C

5.2 Recommendations for future work

This thesis has shown that temperature affects bubble sizes and is more evident at low temperatures. Several authors have proposed several methods to improve the adverse effects of low temperatures on concentrate yield and grade, such as additional cleaning stage, heating the pulp, or increased reagent addition. Further research could be conducted to investigate the effect of changes in the operation parameters (frother dosage, superficial gas velocity) on bubble size at low temperatures. A design of experiments (DOE) with response surface methodology (RSM) can be used to identify optimal conditions in order to minimize the Sauter mean diameter and develop a model. The obtained model could then be used to predict the bubble sizes at low temperatures at low and high factor levels.

REFERENCES

Ata, S. (2012). Phenomena in the froth phase of flotation—A review. *International Journal of Mineral Processing*, *102*, 1-12.

Bailey, R., & Whelan, P. F. (1957). Influence of pulp temperature on the froth flotation of four British fine coals. *J. Inst. Fuel*, *25*, 304-307.

Bournival, G., Pugh, R. J., & Ata, S. (2012). Examination of NaCl and MIBC as bubble coalescence inhibitor in relation to froth flotation. *Minerals Engineering*, *25*(1), 47-53.

Bhattacharya, S., & Pascoe, R.D. (2004). Effect of temperature on coal flotation performance—A review. *Mineral Processing and Extractive Metallurgy Review*, *26*(1), 31-61.

Bhattacharya, S., Roy, J., & Sinha, S. (2002). Effect of seasonal variation in temperature on coal flotation. *XIV ICPC*, 359-364.

Cappuccitti, F., & Nesset, J. E. (2009, August). Frother and collector effects on flotation cell hydrodynamics and their implication on circuit performance. In *Proceedings 48th Conference of Metallurgists of CIM. Sudbury* (pp. 169-180).

Chander, S., & Nagaraj, D. R. (2007). FLOTATION Flotation Reagents.

Chipfunhu, D., Bournival, G., Dickie, S., & Ata, S. (2019). Performance characterisation of new frothers for sulphide mineral flotation. Minerals Engineering, 131, 272-279.

Cho, Y. S., & Laskowski, J. S. (2002). Effect of flotation frothers on bubble size and foam stability. *International Journal of Mineral Processing*, *64*(2-3), 69-80.

Comley, B. A., Harris, P. J., Bradshaw, D. J., & Harris, M. C. (2002). Frother characterisation using dynamic surface tension measurements. *International Journal of Mineral Processing*, *64*(2-3), 81-100.

Corin, K. C., & O'connor, C. T. (2014). A proposal to use excess Gibbs energy rather than HLB number as an indicator of the hydrophilic–liphophilic behavior of surfactants. *Minerals Engineering*, *58*, 17-21.

Deglon, D. A., Egya-Mensah, D., & Franzidis, J. P. (2000). Review of hydrodynamics and gas dispersion in flotation cells on South African platinum concentrators. Minerals Engineering, 13(3), 235-244.

Derjaguin, B. V., & Dukhin, S. S. (1993). Theory of flotation of small and medium-size particles. Progress in Surface Science, 43(1-4), 241-266.

Drzymala, J., & Kowalczuk, P. B. (2018). Classification of flotation frothers. *Minerals*, *8*(2), 53.

Drzymala, J., Kliszowska, K., & Ratajczak, T. (2022). Theoretical and Experimental Aspects of Influence of Temperature on Kinetics of Carbonaceous Materials Froth Flotation. *Mineral Processing and Extractive Metallurgy Review*, *43*(4), 422-426.

Elmahdy, A.M., & Finch, J. A. (2013). Effect of frother blends on hydrodynamic properties. *International Journal of Mineral Processing, 123, 60-63*

Farrokhpay, S. (2011). The significance of froth stability in mineral flotation—A review. *Advances in colloid and interface science*, *166*(1-2), 1-7.

Finch, J. A., Nesset, J. E., & Acuña, C. (2008). Role of frother on bubble production and behaviour in flotation. *Minerals Engineering*, *21*(12-14), 949-957.

Finch, J. A., & Zhang, W. (2014). Frother function–structure relationship: Dependence of CCC_{95} on HLB and the H-ratio. *Minerals Engineering*, *61*, 1-8.

Franzidis, J. P., & Harris, M. C. (2010). Froth recovery factor–what is it and why is it so difficult to measure?. *Canadian Metallurgical Quarterly*, *49*(4), 337-344.

Fuerstenau, M. C., Jameson, G. J., & Yoon, R. H. (Eds.). (2007). *Froth flotation: a century of innovation*. SME.

Gélinas, S., & Finch, J. A. (2007). Frother analysis: Some plant experiences. *Minerals Engineering*, *20*(14), 1303-1308.

Gomez, C. O., & Finch, J. A. (2007). Gas dispersion measurements in flotation cells. International Journal of Mineral Processing, 84(1-4), 51-58.

Grau, R. A., Laskowski, J. S., & Heiskanen, K. (2005). Effect of frothers on bubble size. *International Journal of Mineral Processing*, *76*(4), 225-233.

Gupta, A. K., Banerjee, P. K., Mishra, A., & Satish, P. (2007). Effect of alcohol and polyglycol ether frothers on foam stability, bubble size and coal flotation. *International Journal of Mineral Processing*, *82*(3), 126-137.

Gupta, A., & Yan, D. S. (2016). *Mineral processing design and operations: an introduction*. Elsevier.

Harris, P. J. (1982). Frothing phenomena and frothers. *South African Institute of Mining and Metallurgy, Principles of Flotation,* 237-250.

Haryono, D., Nugraha, H., Al Huda, M., Taruno, W. P., & Harjanto, S. (2017). The Effect of Flotation Reagents Addition (MIBC and PAX) on the Relative Permittivity Value Using 2-Electrode Capacitance Sensor. *Procedia engineering*, *170*, 369-372.

Hernandez-Aguilar, J. R., Rao, S. R., & Finch, J. A. (2005). Testing the k–Sb relationship at the microscale. *Minerals Engineering*, *18*(6), 591-598.

Hofmeier, U., Yaminsky, V. V., & Christenson, H. K. (1995). Observations of solute effects on bubble formation. *Journal of colloid and interface science*, *174*(1), 199-210.

James, C. J., Mulcahy, D. E., & Steel, B. J. (1984). Viscometer calibration standards: Viscosities of water between 0 and 60 degrees C and of selected aqueous sucrose solutions at 25 degrees C from measurements with a flared capillary viscometer. *Journal of Physics D: Applied Physics*, *17*(2), 225.

Khoshdast, H., & Sam, A. (2011). Flotation frothers: review of their classifications, properties, and preparation. *The Open Mineral Processing Journal*, *4*(1), 25-44.

Klassen, V. I. (1963). Coal flotation. *Moscow, Gosgortiekhizdat, and Katowice, Russia, Slask (in Russian and Polish).*

Klimpel, R. R., & Hansen, R. D. (1988). The interaction of flotation chemistry and size reduction in the recovery of a porphyry copper ore. *International Journal of Mineral Processing*, *22*(1-4), 169-181.

Klimpel, R. R., & Isherwood, S. (1991). Some industrial implications of changing frother chemical structure. *International journal of mineral processing*, *33*(1-4), 369-381

Kracht, W., & Finch, J. A. (2009). Bubble break-up and the role of frother and salt. *International Journal of Mineral Processing*, *92*(3-4), 153-16

Kyzas, G. Z., Lazaridis, N. K., & Matis, K. A. (2019). Flotation: Recent innovations in an interesting and effective separation process. In *Interface Science and Technology* (Vol. 30, pp. 15-42). Elsevier.

Kyzas, G. Z., & Mitropoulos, A. C. (Eds.). (2019). *Advanced Low-Cost Separation Techniques in Interface Science*. Academic Press

Kowalczuk, P. B. (2013). Determination of critical coalescence concentration and bubble size for surfactants used as flotation frothers. *Industrial & Engineering Chemistry Research*, *52*(33), 11752-11757.

Laskowski, J. (2001). *Coal flotation and fine coal utilization*. Elsevier.

Laskowski J. S., 2003. Fundamental properties of flotation frothers, Proceedings of the 22nd International Mineral Processing Congress (IMPC), Edited by Lorenzen L., Bradshaw D., Cape Town, South Africa, 29 Sept – 3 Oct, pp 788-797.

Laskowski, J. S. (2004). Testing flotation frothers. *Fizykochemiczne Problemy Mineralurgii/Physicochemical Problems of Mineral Processing*, *38*, 13-22.

Lazarov, D., Alexandrova, L., & Nishkov, I. (1994). Effect of temperature on the kinetics of froth flotation. *Minerals engineering*, *7*(4), 503-509.

López-Saucedo, F., Uribe-Salas, A., Pérez-Garibay, R., & Magallanes-Hernández, L. (2012). Gas dispersion in column flotation and its effect on recovery and grade. *Canadian Metallurgical Quarterly*, *51*(2), 111-117.

Nagaraj, D. R., & Ravishankar, S. A. (2007). Flotation reagents—A critical overview from an industry perspective. *Froth flotation: A century of innovation*, 375-424.

Nassif, M., Finch, J. A., & Waters, K. E. (2014). Determining frother-like properties of process water in bitumen flotation. *Minerals Engineering*, *56*, 121-128.

Navarra, A., Acuna, C., & Finch, J. A. (2009). Impact of frother on the terminal velocity of small bubbles. *International Journal of Mineral Processing*, *91*(3-4), 68-73.

Nesset, J. E. (2011). Modeling the Sauter mean bubble diameter in mechanical forced-air flotation machines.

Nesset, J. E., Finch, J. A., & Gomez, C. O. (2007, March). Operating variables affecting the bubble size in forced-air mechanical flotation machines. In *Proceedings AusIMM 9th Mill Operators' Conference, Fremantle, Australia* (pp. 66-75).

O'Connor, C. T., Dunne, R. C., & De Sousa, A. M. R. B. (1984). The effect of temperature on the flotation of pyrite. *J. S. Afr. Inst. Min. Metall.*, *84*(12), 389-394.

Quinn, J. J., Kracht, W., Gomez, C. O., Gagnon, C., & Finch, J. A. (2007). Comparing the effect of salts and frother (MIBC) on gas dispersion and froth properties. *Minerals Engineering*, *20*(14), 1296-1302.

Quinn, J. J., Sovechles, J. M., Finch, J. A., & Waters, K. E. (2014). Critical coalescence concentration of inorganic salt solutions. *Minerals Engineering*, *58*, 1-6.

Rao, S. R., & Leja, J. (2004). *Surface chemistry of froth flotation: Reagents and mechanisms*.

Sovechles, J. M., Lepage, M. R., Johnson, B., & Waters, K. E. (2016). Effect of gas rate and impeller speed on bubble size in frother-electrolyte solutions. *Minerals Engineering*, *99*, 133-141.

Sovechles, J. M., & Waters, K. E. (2015). Effect of ionic strength on bubble coalescence in inorganic salt and seawater solutions. *AIChE Journal*, *61*(8), 2489-2496.

Sun, S. C. (1952). Frothing characteristics of pine oils in flotation. *TRANSACTIONS OF THE AMERICAN INSTITUTE OF MINING AND METALLURGICAL ENGINEERS*, *193*(1), 65-71.

Sweet, C., Van Hoogstraten, J., Harris, M., & Laskowski, J. S. (1997, August). The effect of frothers on bubble size and frothability of aqueous solutions. In *Processing of Complex Ores–Proc. 2nd UBC-Mc Gill Int. Symp. Metallurgical Society of CIM, Montreal* (pp. 235-245).

Szyszka, D. (2018). Critical Coalescence Concentration (CCC) for surfactants in aqueous solutions. *Minerals*, *8*(10), 431.

Tan, Y. H., & Finch, J. A. (2016). Frother structure-property relationship: Aliphatic alcohols and bubble rise velocity. *Minerals Engineering*, *96*, 33-38.

Tan, S. N., Pugh, R. J., Fornasiero, D., Sedev, R., & Ralston, J. (2005). Foaming of polypropylene glycols and glycol/MIBC mixtures. *Minerals Engineering*, *18*(2), 179-188.

Tan, Y. H., Zhang, W., & Finch, J. A. (2018). Frother structure-property relationship: Effect of polyethylene glycols on bubble rise velocity. *Minerals Engineering*, *116*, 56-61.

Tsiperovich, M. V. and Sorokin, A. F. (1964). Study of the Action of Organic Compounds in Coal Flotation, Moscow, Russia, Nedra (in Russian).

Wills, B. A., & Finch, J. A. (2016). Froth flotation, Chapter 12, Wills' Mineral Processing Technology (8th).

Zhang, W. (2014). Evaluation of effect of viscosity changes on bubble size in a mechanical flotation cell. *Transactions of Nonferrous Metals Society of China*, *24*(9), 2964-2968.

Zhang, W., Zhu, S., & Finch, J. A. (2013). Frother partitioning in dual-frother systems: Development of analytical technique. *International Journal of Mineral Processing*, *119*, 75-82.

Zhou, X., Jordens, A., Cappuccitti, F., Finch, J. A., & Waters, K. E. (2016). Gas dispersion properties of collector/frother blends. *Minerals Engineering*, *96*, 20-25.